Distribution of ^{210}Pb and ^{210}Po in the Arctic water column during the 2007 sea-ice minimum: particle export in the ice-covered basins

Montserrat Roca-Martí [a,b], Viena Puigcorbé [c], Jana Friedrich [d,e], Michiel Rutgers van der Loeff [e], Benjamin Rabe [e], Meri Korhonen [f], Patricia Cámara-Mor [a], Jordi Garcia-Orellana [a], and Pere Masqué [a,c,g]

Affiliations:

[a] Institut de Ciència i Tecnologia Ambientals & Departament de Física, Universitat Autònoma de Barcelona, 08193 Bellaterra, Spain

[b] Woods Hole Oceanographic Institution, Woods Hole MA 02543, USA

[c] School of Science, Centre for Marine Ecosystems Research, Edith Cowan University, Joondalup WA 6027, Australia

[d] Helmholtz Zentrum Geesthacht Centre for Materials and Coastal Research, 21502 Geesthacht, Germany

[e] Alfred-Wegener-Institut Helmholtz-Zentrum für Polar- und Meeresforschung, 27570 Bremerhaven, Germany

[f] Finnish Meteorological Institute, 00560 Helsinki, Finland

[g] Oceans Institute and School of Physics, The University of Western Australia, Crawley WA 6009, Australia

ABSTRACT

^{210}Pb and ^{210}Po are naturally occurring radionuclides that are commonly used as a proxy for particle and carbon export. In this study, the distribution of the ^{210}Po/^{210}Pb pair was investigated in the water column of the Barents, Kara and Laptev Seas and the Nansen, Amundsen and Makarov Basins in order to understand the particle dynamics in the Arctic Ocean during the 2007 sea-ice minimum (August-September). Minimum activities of total ^{210}Pb and ^{210}Po were found in the upper and lower haloclines (approx. 60-130 m), which are partly attributed to particle scavenging over the shelves, boundary current transport and subsequent advection of the water with low ^{210}Pb and ^{210}Po activities into the central Arctic. Widespread and substantial (>50%) deficits of ^{210}Po with respect to ^{210}Pb were detected from surface waters to 200 m on the shelves, but also in the basins. This was particularly important in the Makarov Basin where, despite very low chlorophyll-a levels, estimates of annual new primary production were three times higher

than in the Eurasian Basin. In the Nansen, Amundsen and Makarov Basins, estimates of annual new primary production correlated with the deficits of ^{210}Po in the upper 200 m of the water column, suggesting that in situ production and subsequent export of biogenic material were the mechanisms that controlled the removal of ^{210}Po in the central Arctic. Unlike ^{210}Po, ^{234}Th deficits measured during the same expedition were found to be very small and not significant below 25 m in the basins (Cai et al., 2010), which indicates, given the shorter half-life of ^{234}Th, that particle export fluxes in the central Arctic would have been higher before July-August in 2007 than later in the season.

Keywords:

Particle export, annual new primary production, scavenging, ^{210}Po/^{210}Pb, Arctic Ocean, 2007 sea-ice minimum

Highlights:

- Largest dataset of ^{210}Pb and ^{210}Po in the Arctic Ocean to date
- Minimum ^{210}Pb and ^{210}Po activities in the halocline reflect scavenging on the shelf
- Potential use of the ^{210}Po/^{210}Pb proxy as an indicator of annual new primary production
- Substantial deficits of ^{210}Po in surface and subsurface waters of the Makarov Basin
- Higher particle export in the central Arctic before July-August in 2007

1. Introduction

The Arctic Ocean is undergoing rapid changes in response to global warming, including a rapid sea-ice retreat (e.g. Stroeve et al., 2012). During the past 10 years, the Arctic sea-ice extent has experienced two record minima in September 2007 and 2012, related to anomalously high temperatures and southerly winds (Comiso et al., 2008), or intense cyclone events (Parkinson and Comiso, 2013). Sea ice has also thinned and lost volume (Kwok et al., 2009; Laxon et al., 2013; Renner et al., 2014). The freshwater storage in the upper Arctic Ocean has concurrently increased, primarily due to a reduction in the average salinity in the layer between the surface and the lower halocline and, to a lesser extent, due to the thickening of that layer (Haine et al., 2015; Rabe et al., 2014, 2011). These changes have been accompanied by an increase in upper ocean stratification

(Korhonen et al., 2013). This scenario impacts primary production (e.g. Ardyna et al., 2014; Arrigo and van Dijken, 2015), marine ecosystems (Wassmann et al., 2011) and pelagic-benthic coupling (Wassmann and Reigstad, 2011), but there are many uncertainties due to the limitations in obtaining in situ data. Therefore, impacts on biogeochemical cycles in the Arctic remain poorly understood, including the transport of particles to deep waters and its implications for carbon export (Reid et al., 2009; Tremblay et al., 2015; Wassmann, 2011).

The present understanding is that particle and carbon export from the upper water column to depth is widely heterogeneous in the Arctic, being substantially higher on the shelves than in the basins in consistency with the distribution of primary production (Findlay et al., 2015; Honjo et al., 2010; Randelhoff and Guthrie, 2016; Wassmann et al., 2004). In the late summer of 2007, the time of the present study, deficits of ^{234}Th with respect to its parent, ^{238}U, in the upper 100 m of the water column were basically restricted to the Arctic shelves and continental margins (Cai et al., 2010); in the deep basins (>80ºN), very small ^{234}Th deficits were measured in the upper 25 m and ^{234}Th/^{238}U ratios were indistinguishable from 1 at deeper depths, indicating very small particle export in the central Arctic. This low export is in line with previous studies conducted in the central Arctic during the summer season (see compilation of ^{234}Th flux data in Roca-Martí et al., 2016), although there are exceptions, for instance, in the Canada Basin (e.g. Baskaran et al., 2003; Ma et al., 2005).

The natural radionuclides ^{210}Pb (half-life, $T_{1/2}$ = 22.3 years) and ^{210}Po ($T_{1/2}$ = 138.4 days) have been widely used as particle tracers in the marine environment (e.g. Bacon et al., 1988, 1976; Cochran and Masqué, 2003), but their application in the Arctic is scarce (Moore and Smith, 1986; Roca-Martí et al., 2016; Smith et al., 2003; Smith and Ellis, 1995). Both have a strong affinity for particle surfaces, but ^{210}Po is also incorporated into the cytoplasm of bacteria and phytoplankton (Cherrier et al., 1995; Fisher et al., 1983) and is preferentially assimilated by zooplankton with respect to ^{210}Pb (Stewart and Fisher, 2003). When sinking of biogenic particles occurs, the different biogeochemical behaviours of ^{210}Pb and ^{210}Po create a deficit of the latter in the ocean surface that can be used to estimate particulate organic carbon (POC) sinking fluxes (see review by Verdeny et al., 2009). The ^{210}Po/^{210}Pb pair has, potentially, some advantages over the most commonly used proxy for POC export, the ^{234}Th/^{238}U pair, when studying export on a

seasonal scale: ^{210}Po has a stronger preference for POC than ^{234}Th (Friedrich and Rutgers van der Loeff, 2002) and, with a mean life of 200 days, ^{210}Po integrates a time scale of several months, while ^{234}Th (mean life of 35 days) misses events that had occurred more than one month before sampling (Stewart et al., 2007a; Verdeny et al., 2009).

Here, we examine the distribution of ^{210}Pb and ^{210}Po (total and particulate) on three shelves (Barents, Kara and Laptev) and in three deep basins (Nansen, Amundsen and Makarov) of the Arctic Ocean in order to investigate the processes governing the dynamics of particles and the particle export around the time of the sea-ice minimum in summer 2007. This is combined with information on physical characteristics of the study areas, estimates of annual new primary production and the export production derived from ^{234}Th data from the same expedition (Cai et al., 2010).

2. Materials and methods

2.1. Study area

Seawater samples were collected during the ARK-XXII/2 expedition that took place from 28 July to 7 October in 2007 along the shelves of the Barents, Kara and Laptev Seas and the Nansen, Amundsen and Makarov Basins (R/V Polarstern, Schauer, 2008). Stations have been classified into three categories according to the water depth (Table 1, shelf: <350 m; slope: 350-1050 m; basin: >1050 m), and divided into five sections (S1-S5, see Figure 1), similarly to Cai et al. (2010).

2.2. ^{210}Pb and ^{210}Po

Pb-210 and ^{210}Po activities were measured in the dissolved and particulate fractions in the upper ~500 m of the water column, while only total activities were determined for deeper samples (Table S1). Surface seawater (10 m) was sampled at 50 stations (Table 1) using the ship seawater intake. Vertical profiles were collected at 17 stations (Table 1) using Niskin bottles attached to a conductivity-temperature-depth (CTD) rosette sampler. The sample volumes were about 20 L (dissolved and total) and 40 to 160 L (particulate). Samples were filtered through 1 μm pore-size Nuclepore filters (142 mm, Whatman) to separate the dissolved and particulate fractions. After filtration, the filters were dried at room temperature and stored for later processing at the Alfred Wegener Institute (AWI). Samples for the analyses of the total and dissolved fractions were acidified with 20 mL

concentrated HNO_3 immediately after collection and filtration, respectively, and spiked with known amounts of ^{208}Po ($T_{1/2}$ = 2.9 years) and stable Pb. After addition of $FeCl_3$ as a carrier and vigorous stirring, samples were allowed to equilibrate for about 24 h. Pb and Po were then co-precipitated with $Fe(OH)_3$ by adjusting the pH to ~8.5 with ammonium hydroxide solution. After a few hours, supernatants were removed carefully by decantation and samples were centrifuged. Precipitates were transferred to plastic bottles and stored until further analyses at AWI.

Pb-210 and ^{210}Po were determined following the method of Fleer and Bacon (1984), based on the procedure of Flynn (1968). Filters (i.e. particulate fraction) were spiked with ^{208}Po and stable Pb and digested using a microwave with a mixture of HNO_3, HF and H_2O_2 (10, 0.3 and 2 mL, respectively). Pb and Po isotopes were then co-precipitated with $Fe(OH)_3$ as described for water samples. Iron precipitates were dissolved in 0.5 M HCl and ascorbic acid was added to the solutions to reduce Fe^{3+} to Fe^{2+} before placing the silver discs and hence allow the auto-deposition of Po (80ºC, >4 hours). The silver discs were then counted for Po by alpha spectrometry using silicon surface barrier alpha detectors (EG&G Ortec, USA) for about seven days to achieve counting statistics <5%. Samples were re-spiked with ^{209}Po ($T_{1/2}$ = 125 years) and stored for 15 to 26 months in 8 M HNO_3 for later determination of ^{210}Pb via ^{210}Po ingrowth. Samples were plated for Po as described above and counted once more by alpha spectrometry. Pb-210 and ^{210}Po activities at sampling time were calculated applying appropriate ingrowth and decay corrections (Fleer and Bacon, 1984). The chemical yield of stable Pb was determined by inductively coupled plasma-optical emission spectrometry (ICP-OES, Thermo Fisher Scientific, USA). The activity uncertainties, which account for counting, detector background, spike activities and sample volume, were on average 5% for ^{210}Pb and 9% for ^{210}Po for the dissolved and total fractions, and 5% for ^{210}Pb and 15% for ^{210}Po for the particulate fraction. The greater uncertainties of ^{210}Po are due to the time elapsed between sampling and the first Po plating (range: 55-117 days; median: 78 days).

The AWI laboratory participated in the ^{210}Pb and ^{210}Po inter-calibration exercise organized by GEOTRACES in 2008-2009 (Church et al., 2012). This study recommended a minimum sample activity of 0.1 dpm for both radionuclides. In this work, the reported activities of ^{210}Pb and ^{210}Po are always higher than 0.1 dpm for the dissolved and total fractions, while the particulate activities of both radionuclides are below this

154 threshold in about 10% of the samples. The complete ^{210}Pb and ^{210}Po dataset can be found
155 in Table S1 (Supplemental Material) and is available at PANGAEA (Friedrich, 2011).

156 **2.3. CTD observations and nutrients**

157 Profiles of temperature and salinity in the water column were obtained using a CTD
158 system with a Carousel Water Sampler (Sea-Bird Electronics Inc., USA). Salinity was
159 calibrated using discrete samples from the rosette, and processed with an on-board
160 salinometer. Discrete nutrient water samples from the rosette were processed using a
161 Technicon TRAACS 800 continuous flow auto-analyser and standards previously
162 prepared on land. Details of the measurements and processing are described in Schauer
163 (2008). The data are published in Laan et al. (2008), Wisotzki and Bakker (2008) and
164 Schauer and Wisotzki (2010).

165 **2.4. Annual new primary production**

166 New primary production during the productive season after the Arctic winter (from April
167 to sampling time) was calculated by using estimates of the winter mixed layer depth and
168 the seasonal nutrient uptake based on measurements made during the ARK-XXII/2
169 expedition, following Rudels et al. (1996) and Korhonen et al. (2013). The method
170 interpolates data as in Reiniger and Ross (1968) and is described in detail in Boetius et
171 al. (2013) and Fernández-Méndez et al. (2015). The winter mixed layer depth was
172 estimated by the temperature minimum below the summer mixed layer (August-
173 September 2007), which is assumed to be a remnant of the previous winter convection
174 and homogenization (Rudels et al., 1996). Briefly, in the summer season the net ice melt
175 and warming due to solar radiation both make the surface layer less dense. Because the
176 freshening and warming do not reach below the shallow summer mixed layer, the
177 temperature minimum below this layer and the summer halocline is very likely a remnant
178 of the previous winter mixed layer. Then, the total inventory of nutrients used up since
179 the previous winter is estimated by integrating the difference between the nutrient
180 concentration profiles and the nutrient concentrations at the winter mixed layer depth
181 measured in late summer in the vertical from the surface to the winter mixed layer depth.
182 The annual total inorganic nitrogen (nitrite+nitrate), phosphate and silicate uptake was
183 then converted to carbon units using the Redfield-Brzezinski ratio 106C:16N:15Si:1P
184 (Brzezinski, 1985; Redfield et al., 1963), as done by Boetius et al. (2013), Ulfsbo et al.

(2014) and Fernández-Méndez et al. (2015). The elemental stoichiometry 106C:16N was confirmed for the central Arctic by analysis of suspended particulate organic matter collected during several research programmes (n = 255; Frigstad et al., 2014).

Annual new primary production has been only estimated at those stations located in the basins (where ^{210}Pb and ^{210}Po vertical profiles were taken; Table 2). This method assumes that lateral inputs of nutrients from rivers and shelves to surface and subsurface waters in the deep central Arctic (>78ºN) have a limited impact on the annual new primary production estimates because the horizontal distance between the shelves and the basin stations is too large to be covered from the winter mixing to the time of sampling with published rates of transport (Ekwurzel et al., 2001; Rutgers van der Loeff et al., 2018). This method does not take into account nitrification, phosphorus remineralization and silica dissolution occurring at or above the winter mixed layer depth during the season. Ulfsbo et al. (2014) found good agreement when comparing this method (using nitrogen and phosphate) to three alternative approaches using concurrent observations during late summer.

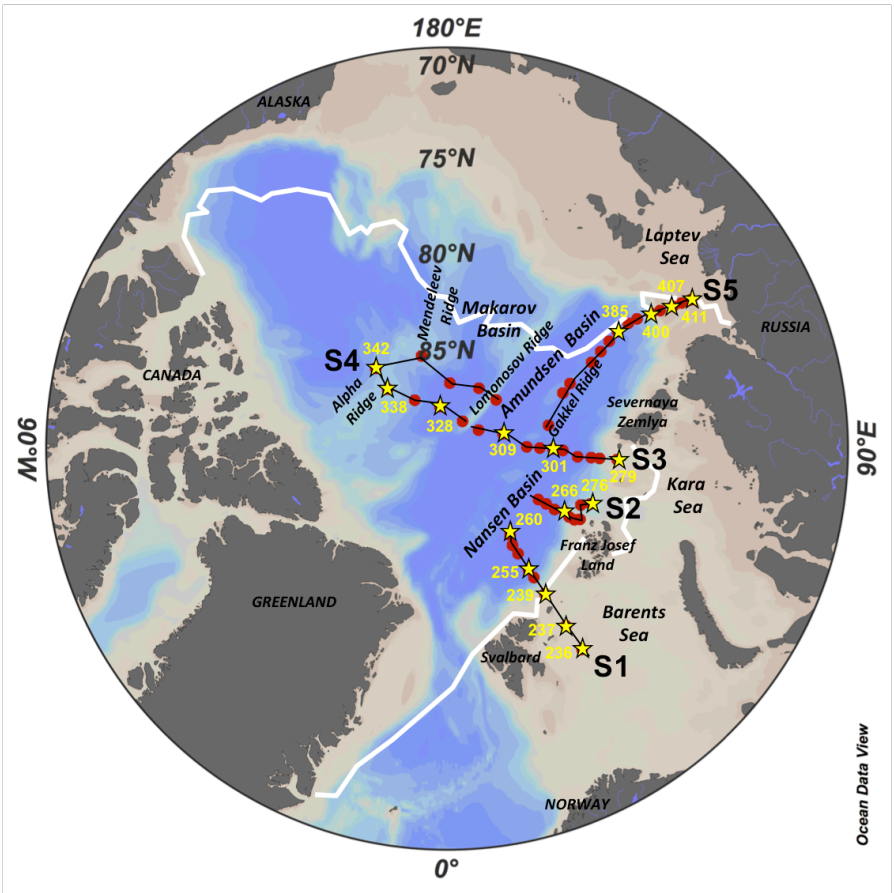

201 **Figure 1:** Location of the stations sampled for surface waters (red dots) and vertical profiles (yellow stars
202 with station numbers) during the ARK-XXII/2 cruise (July-October 2007). The study area is divided into
203 five sections: S1, stations 236-260; S2, stations 261-276; S3, stations 279-312; S4, stations 320-363; S5,
204 stations 371-411. The contour white line represents the minimum sea-ice extent in September 2007
205 (http://www.meereisportal.de).

Table 1: Coordinates, sampling date and water column depth (down to the seafloor) of the stations sampled for ^{210}Pb and ^{210}Po analyses during the ARK-XXII/2 expedition. It is indicated whether the stations were only sampled for surface seawater (10 m) or depth profiles were collected (n refers to the number of samples, see Table S1 for further details). Stations have been classified into sections (S1-S5) and areas (location and shelf/slope/basin, see text for further details).

Section	Station	Long. (ºE)	Lat. (ºN)	Date (2007)	Samples collected	Water depth (m)	Area
S1	236	33.98	77.50	31 Jul.	Depth profile (n = 7)	196	Barents Shelf
	237	33.97	79.00	31 Jul.	Depth profile (n = 7)	272	Barents Shelf
	239	34.00	80.99	1 Aug.	Depth profile (n = 7)	224	Barents Shelf
	249	33.98	82.00	2 Aug.	Surface seawater	2281	Nansen Basin
	255	33.89	82.52	4 Aug.	Depth profile (n = 11)	3135	Nansen Basin
	257	34.05	83.50	5 Aug.	Surface seawater	3958	Nansen Basin
	258	34.00	84.00	6 Aug.	Surface seawater	4055	Nansen Basin
	260	36.08	84.51	8 Aug.	Depth profile (n = 10)	4054	Nansen Basin
S2	261	60.92	84.64	11 Aug.	Surface seawater	3846	Nansen Basin
	263	60.96	84.17	11 Aug.	Surface seawater	3713	Nansen Basin
	264	60.43	83.65	12 Aug.	Surface seawater	3512	Nansen Basin
	266	61.81	83.12	14 Aug.	Depth profile (n = 13)	3011	Nansen Basin
	268	60.81	82.81	14 Aug.	Surface seawater	1609	Nansen Basin
	271	60.80	82.50	15 Aug.	Surface seawater	327	Barents Shelf
	272	61.99	82.25	15 Aug.	Surface seawater	231	Barents Shelf
	274	67.10	82.52	16 Aug.	Surface seawater	1176	Nansen Basin
	276	68.95	82.09	17 Aug.	Depth profile (n = 8)	680	Kara Slope
S3	279	86.23	81.24	19 Aug.	Depth profile (n = 7)	336	Kara Shelf
	285	86.34	82.14	20 Aug.	Surface seawater	724	Kara Slope
	290	86.44	82.58	21 Aug.	Surface seawater	2071	Nansen Basin
	295	86.30	83.27	22 Aug.	Surface seawater	3357	Nansen Basin
	299	89.06	84.05	23 Aug.	Surface seawater	3694	Nansen Basin
	301	89.76	84.56	24 Aug.	Depth profile (n = 14)	3758	Nansen Basin
	303	90.23	85.25	25 Aug.	Surface seawater	3985	Nansen Basin
	306	91.18	85.92	26 Aug.	Surface seawater	4019	Gakkel Ridge (basin)

	309	104.98	87.04	28 Aug.	Depth profile (n = 14)	4449	Amundsen Basin
	312	120.15	88.12	29 Aug.	Surface seawater	3009	Amundsen Basin
S4	320	150.33	88.41	31 Aug.	Surface seawater	1952	Makarov Basin
	328	-170.33	87.82	2 Sept.	Depth profile (n = 13)	3992	Makarov Basin
	333	-146.39	87.03	4 Sept.	Surface seawater	3285	Makarov Basin
	338	-134.96	85.69	6 Sept.	Depth profile (n = 11)	1570	Makarov Basin
	342	-138.30	84.50	7 Sept.	Depth profile (n = 12)	2289	Makarov Basin
	349	-164.55	85.07	9 Sept.	Surface seawater	1996	Makarov Basin
	352	177.54	86.64	10 Sept.	Surface seawater	4005	Makarov Basin
	358	151.96	86.51	11 Sept.	Surface seawater	1459	Makarov Basin
	363	134.92	86.47	13 Sept.	Surface seawater	3991	Amundsen Basin
S5	371	102.73	84.66	16 Sept.	Surface seawater	4271	Gakkel Ridge (basin)
	377	115.55	83.41	18 Sept.	Surface seawater	4301	Gakkel Ridge (basin)
	379	117.85	82.86	18 Sept.	Surface seawater	4413	Gakkel Ridge (basin)
	382	120.72	81.36	19 Sept.	Surface seawater	5343	Gakkel Ridge (basin)
	383	122.21	80.66	19 Sept.	Surface seawater	3902	Gakkel Ridge (basin)
	384	123.46	80.00	20 Sept.	Surface seawater	3653	Gakkel Ridge (basin)
	385	124.36	79.35	20 Sept.	Depth profile (n = 13)	3525	Gakkel Ridge (basin)
	387	124.61	78.64	21 Sept.	Surface seawater	2865	Gakkel Ridge (basin)
	391	124.24	78.13	21 Sept.	Surface seawater	2435	Gakkel Ridge (basin)
	400	123.42	77.37	22 Sept.	Depth profile (n = 11)	1049	Laptev Slope
	404	122.87	76.90	23 Sept.	Surface seawater	94	Laptev Shelf
	407	122.13	76.18	23 Sept.	Depth profile (n = 2)	75	Laptev Shelf
	409	121.77	75.71	23 Sept.	Surface seawater	65	Laptev Shelf
	411	121.36	75.20	24 Sept.	Depth profile (n = 3)	48	Laptev Shelf

209

3. Results and discussion

First, the activities of both radionuclides and the $^{210}Po/^{210}Pb$ ratios in surface waters and vertical profiles are discussed in relation to the area and water masses, and compared to literature data (Section 3.1). Second, the annual new primary production estimates obtained for the basin stations are presented (Section 3.2). Last, total ^{210}Po deficits are discussed in parallel with the annual new primary production estimates and the origin of freshwater in the upper water column (Bauch et al., 2011), and compared to ^{234}Th-derived particle export estimates (Cai et al., 2010) (Section 3.3).

Characteristics of the study area, including hydrography (see Figure S1), sea-ice conditions and nutrient regime can be found in Supplemental Material.

3.1. ^{210}Pb and ^{210}Po in seawater

The activities of ^{210}Pb and ^{210}Po and the $^{210}Po/^{210}Pb$ ratios in surface waters (10 m) and vertical profiles are presented in Figures 2-5 and in Supplemental Material. Vertical profiles were taken down to 25 to 320 m (shelf), 650 to 1015 m (slope), and 1000 to 4365 m (basin).

225

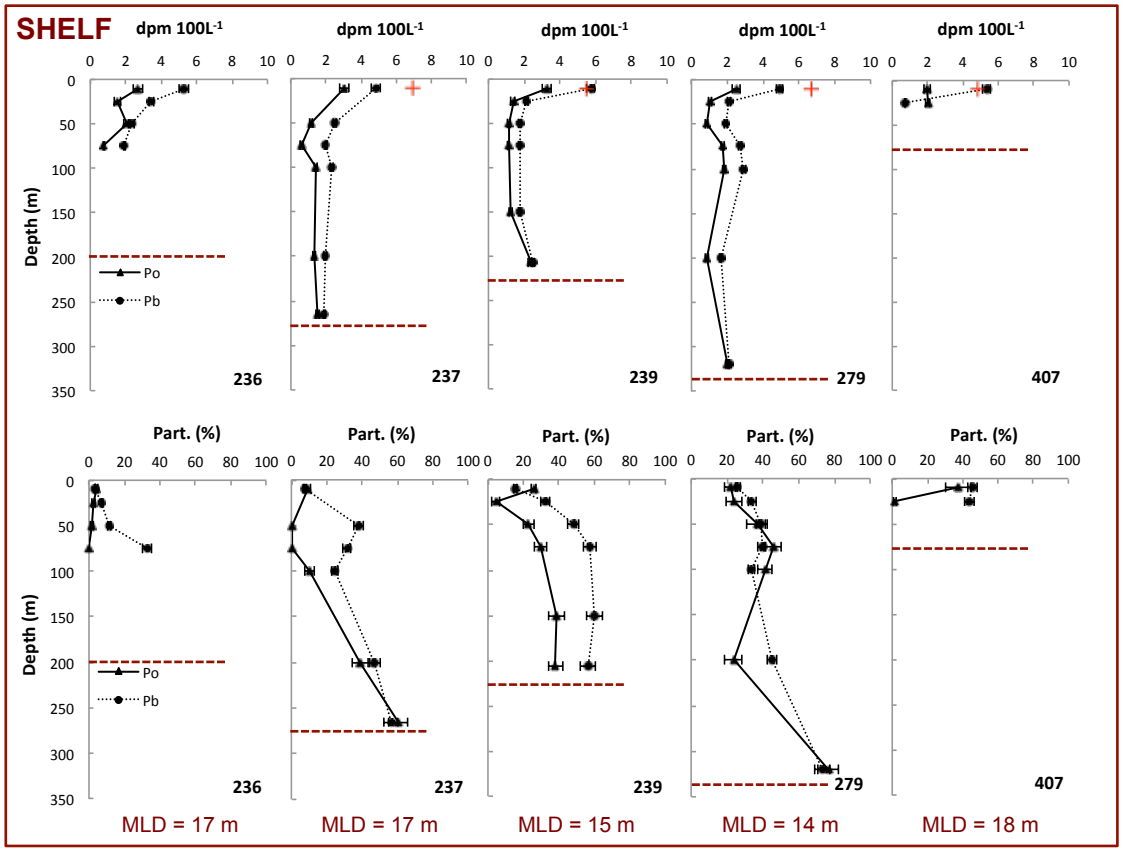
SHELF
dpm 100L-1
Depth (m)
Po
Pb
236
237
239
279
407
Part. (%)
MLD = 17 m
MLD = 17 m
MLD = 15 m
MLD = 14 m
MLD = 18 m

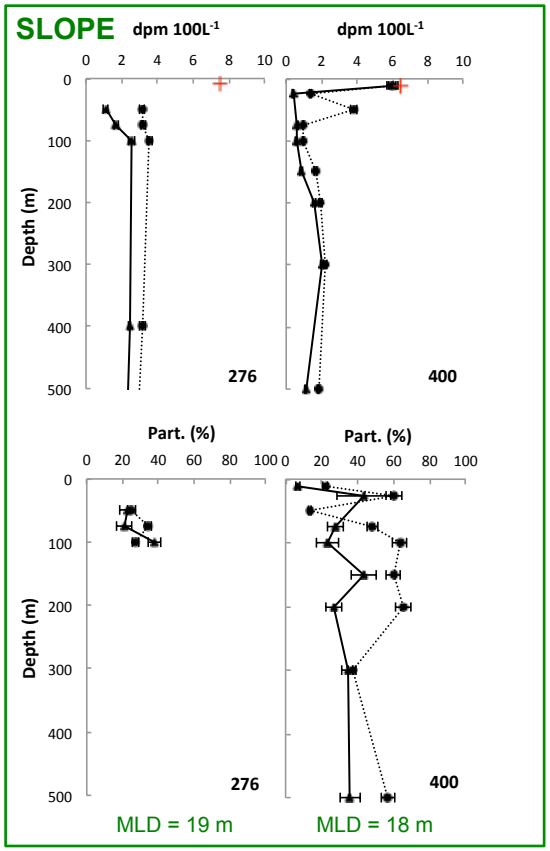
SLOPE
dpm 100L-1
Depth (m)
276
400
Part. (%)
MLD = 19 m
MLD = 18 m

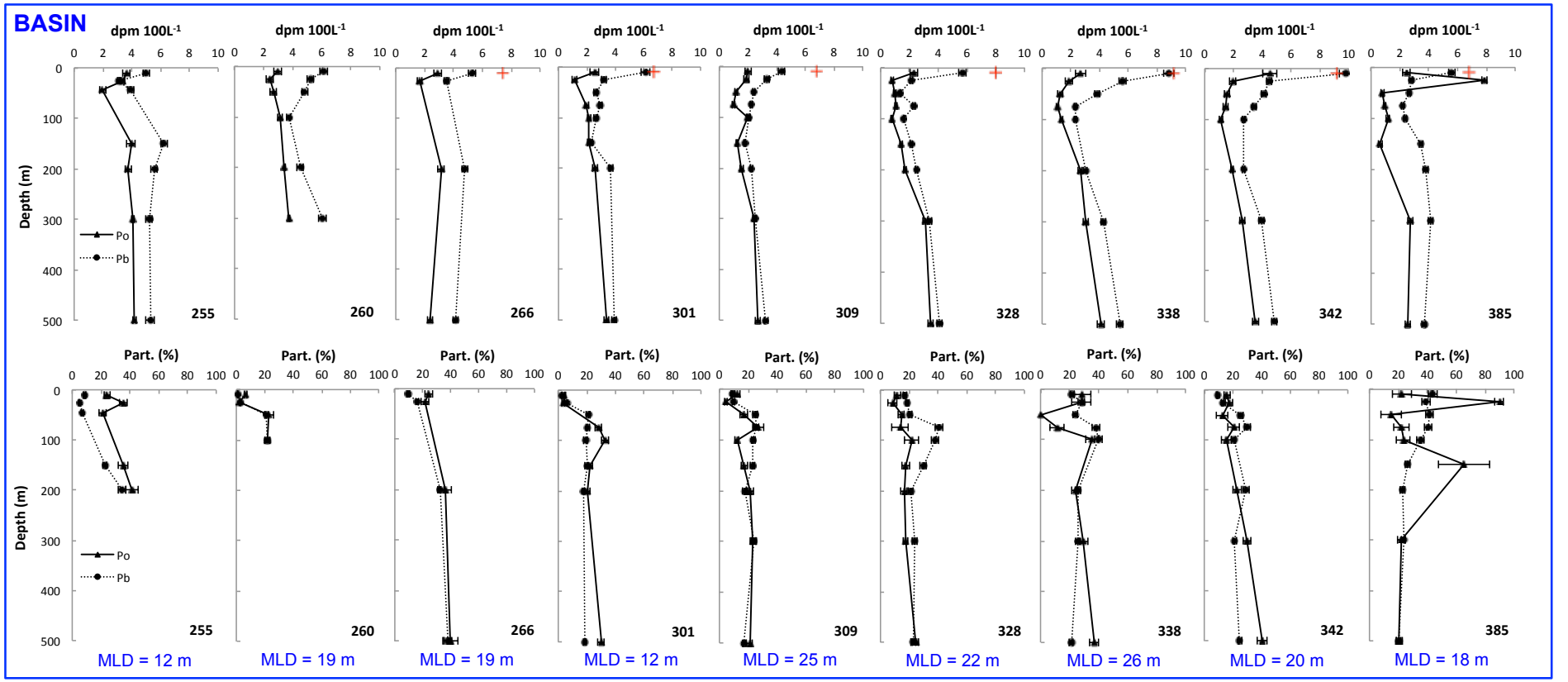

Figure 2: Vertical activity profiles for total ^{210}Po (solid line) and ^{210}Pb (dotted line) and relative contribution of the particulate activities of both radionuclides for the upper 500 m of the water column in the shelf (<350 m), slope (350-1050 m) and basin (>1050 m) environments. The red cross indicates the total activity of ^{226}Ra in surface waters (Rutgers van der Loeff et al., 2012) for comparison with ^{210}Pb activity (see Section 3.1.1). Notice the different scale on the y-axis between the shelf and the slope/basin profiles. The horizontal dashed line in the shelf panel indicates the bottom depth. The mixed layer depth (MLD) for each profile is given at the bottom of the panels. Station 411 is not shown, since the total and particulate activities of ^{210}Pb and ^{210}Po could only be determined at one investigated depth (Table S1, Supplemental Material).

3.1.1. Total ^{210}Pb and ^{210}Po activities and ^{210}Po/^{210}Pb ratios

Total activities of ^{210}Pb and ^{210}Po in the mixed layer (including data from surface stations and vertical profiles) were, on average, 5.8 ± 1.6 dpm 100L^{-1} (n = 39) and 2.6 ± 0.9 dpm 100L^{-1} (n = 38), respectively. The average ^{210}Pb and ^{210}Po activities found below the mixed layer depth in the vertical profiles (3.5 ± 1.7 dpm 100L^{-1} for ^{210}Pb, n = 123; and 2.6 ± 1.7 dpm 100L^{-1} for ^{210}Po, n = 120), show that the mixed layer was enriched in ^{210}Pb with respect to underlying waters.

The ocean surface usually presents higher activities of ^{210}Pb with respect to its parent, ^{226}Ra, due to the atmospheric deposition of ^{210}Pb produced from the decay of ^{222}Rn, representing the major input of ^{210}Pb into the ocean surface (e.g. Nozaki et al., 1980). Considering surface ^{226}Ra data from the same expedition (range: 3.3 to 9.5 dpm 100L^{-1}; Rutgers van der Loeff et al., 2012) and assuming an atmospheric depositional flux of ^{210}Pb of 0.06 dpm cm^{-2} y^{-1} in the Arctic (Huh et al., 1997) the mean residence time of ^{210}Pb in surface waters is 2.0 ± 0.8 years (range: 1.1 to 4.2 years), without significant differences between the shelf and basin environments (Wilcoxon test, $p > 0.05$). This residence time falls in the upper range of previous estimates from diverse oceanic regions including Arctic locations (0.1 to 2.5 years; see references in Masqué et al., 2002 and Smith et al., 2003). Yet, this estimate is very sensitive to the value chosen for the atmospheric flux and does not take into account the role of the sea-ice cover, which intercepts and accumulates a fraction of the atmospheric fluxes during sea-ice transit, releasing them where and when melting occurs (Cámara-Mor et al., 2011; Chen et al., 2012; Masqué et al., 2007; Roberts et al., 1997).

Whereas in surface waters of ice-free areas of the world ocean ^{210}Pb/^{226}Ra ratios are usually larger than 1 as a result of atmospheric deposition, in our study these ratios were >1.0 only at some stations (Table S1, Supplemental Material and Figure 2), where significant amounts of sea-ice meltwater were found (2-8%; Bauch et al., 2011). These stations were located near the ice edge on the Barents and Laptev shelves (239, 407 and 409), and under the sea-ice cover in the Nansen and Makarov Basins (303 and 342). Indeed, considering all stations, there was a positive relationship between the fraction of sea-ice meltwater (Bauch et al., 2011) and ^{210}Pb/^{226}Ra ratios in surface waters ($p < 0.01$; Spearman correlation coefficient, $\rho = 0.63$-0.67 for the two approaches used by Bauch et

al., 2011, n = 20-22; not shown). This suggests a role of sea ice in regulating the amount of atmospherically-derived ^{210}Pb in surface waters, preventing its input where sea ice is present and enhancing ^{210}Pb activities when it melts through the release of accumulated ^{210}Pb in sea ice and/or the direct input of atmospheric ^{210}Pb to seawater. Here, we cannot quantify the effect of sea-ice melt on driving the enrichment of ^{210}Pb in surface waters without considering the concentration of ^{210}Pb in sea ice and its removal by scavenging once released into the ocean. In the case of ^{210}Po, its atmospheric flux to the ocean surface usually accounts for only about 10% of that of ^{210}Pb (Lambert et al., 1982; Baskaran, 2011). However, in the Arctic, the inputs of ^{210}Po to the ocean surface due to sea-ice melt could lead to greater ^{210}Po/^{210}Pb ratios resulting from the ingrowth of ^{210}Po from ^{210}Pb decay in sea ice (range: 0.4-1.0 in sea-ice cores; Masqué et al., 2007; Roca-Martí et al., 2016). Then, a preferential removal of ^{210}Po over ^{210}Pb by particle export in surface waters (Nozaki et al., 1997) may explain the non-significant enrichment of ^{210}Po in the mixed layer.

In the upper halocline (stations 309, 328, 338 and 342), total ^{210}Pb and ^{210}Po activities were on average 2.4 ± 0.6 dpm 100L^{-1} and 1.1 ± 0.2 dpm 100L^{-1} (n = 7), respectively, similarly to the lower halocline, where the activities averaged 2.7 ± 0.7 dpm 100L^{-1} and 1.6 ± 0.7 dpm 100L^{-1} (n = 17), respectively. These values are low in comparison with overlying and intermediate/deep waters (Figure 3). Low total activities of ^{210}Pb and ^{210}Po in the upper halocline were firstly reported for the Canadian Expedition to Study the Alpha Ridge (CESAR; Moore and Smith, 1986), and later for the Makarov and Canada Basins for both ^{210}Pb and ^{210}Po (Smith et al., 2003) or only for ^{210}Pb (Hu et al., 2014; Lepore et al., 2009). This observation was explained by particle scavenging of ^{210}Pb and ^{210}Po at the sediment-water interface over the Chukchi and Beaufort shelves, where the upper halocline is formed, and subsequent advective transport into the interior Arctic (e.g. Rutgers van der Loeff et al., 2012).

Over the Alpha Ridge, the mean ^{210}Pb and ^{210}Po activities in the upper halocline (2.7 ± 0.5 dpm 100L^{-1} and 1.2 ± 0.2 dpm 100L^{-1}, respectively, n = 4, stations 338 and 342) are found to be significantly higher than at the CESAR site (0.75 ± 0.10 dpm 100L^{-1} and 0.52 ± 0.05 dpm 100L^{-1}, respectively; Moore and Smith, 1986; see location in Figure S2). This difference probably derives from temporal variability in the Pacific Water pathways,

294 which are partly controlled by atmospheric circulation patterns (Morison et al., 2012;
295 Steele et al., 2004; Timmermans et al., 2014).

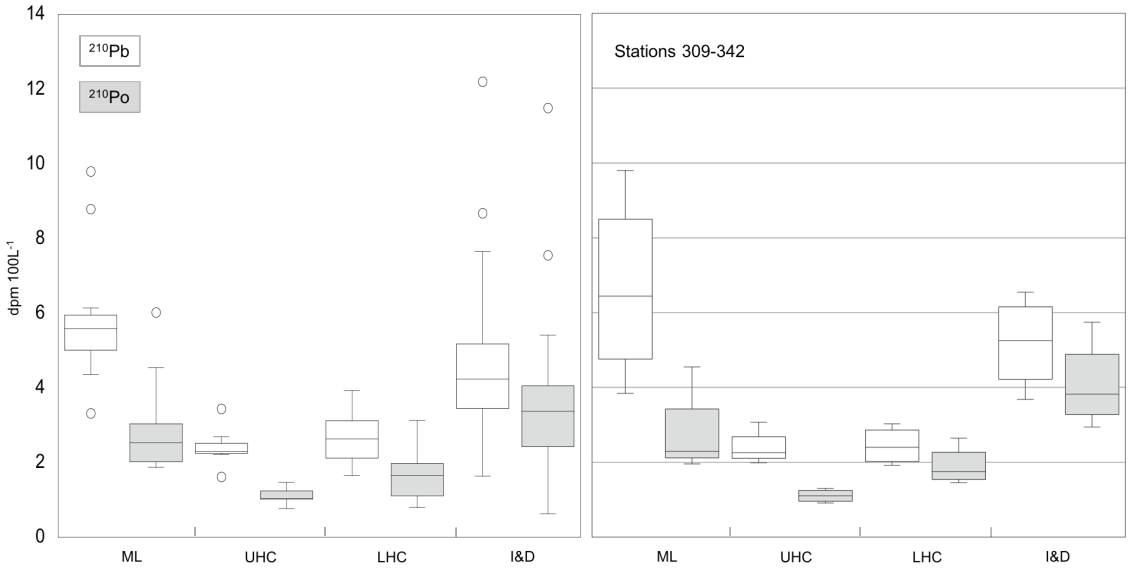

296

297 **Figure 3**: Box plots for total ^{210}Pb and ^{210}Po activities in the mixed layer (ML: surface to MLD), upper
298 halocline (UHC), lower halocline (LHC) and intermediate and deep waters (I&D) obtained from all the
299 vertical profiles (left panel) or only those from stations 309, 328, 338 and 342 (right panel) that showed all
300 water layers (ML, UHC, LHC and I&D). The bottom and top of the boxes mark the 25th and 75th
301 percentiles, respectively, and the middle line represents the median (50th percentile). The lines extending
302 from the bottom and top of the boxes mark the minimum and maximum values. Outliers are displayed as
303 empty circles. Number of samples considered: ML n = 17; UHC n = 7; LHC n = 17; I&D n = 64 (^{210}Po) or
304 65 (^{210}Pb) (left panel); and ML n = 6; UHC n = 7; LHC n = 5; I&D n = 21 (right panel).

305 The lower halocline, in contrast to the upper halocline, is a common feature in the Arctic
306 Ocean, with origin in the Barents Sea or the Nansen Basin (Rudels, 2009). Smith et al.
307 (2003) reported lower ^{210}Pb activities in lower halocline waters formed in the Barents Sea
308 compared to those formed by haline convection in the Nansen Basin. This difference was
309 ascribed to enhanced particle scavenging in the productive and particle-rich Barents Sea,
310 with respect to the Nansen Basin, and removal during boundary current transport into the
311 central Arctic.

312 In summer 2007, ^{210}Pb activities in the lower halocline were higher at the stations located
313 north of the Barents Sea and Franz Josef Land (3.5 ± 0.3 dpm 100L^{-1}, stations 255, 260,
314 266 and 276) than at stations located further east in the Eurasian sector and the Makarov
315 Basin (2.3 ± 0.5 dpm 100L^{-1}, stations 279, 301, 309, 328, 338, 342, 385 and 400) by a
316 factor of 1.5 (Wilcoxon test, $p < 0.01$). Temperature and salinity profiles indicate a
317 potential shelf influence in the lower halocline from station 300 onwards. Yet, we cannot
318 confirm this without data from previous years, since the advective time scales of the lower

halocline from its interaction with the shelves to the central Arctic may be more than a few years (mean of 9.6 ± 4.6 years in Ekwurzel et al., 2001). On the other hand, Laptev shelf waters had an influence on the continental slope driven by the high polynya activity in the Laptev Sea in April 2007 (Bauch et al., 2010). Brine-enriched waters in the surface regime were detected out of the shelf, which could have weakened stratification and enhanced winter convection into the range of the lower halocline. Indeed, a winter mixed layer deeper than 100 m was found on the continental slope at station 400 and surroundings, indicating an influence from the Laptev shelf. Moreover, the halocline around stations 255-276 is generally not influenced by the Barents Sea (Rudels, 2009; Rudels et al., 2004, 1996). Therefore, all these observations suggest that the lower halocline at stations 279-400 had been more affected by shelf processes than at stations 255-276. Thus, enhanced particle scavenging during formation and/or transport of the lower halocline to the Makarov and eastern Eurasian Basins would explain the lower activities of ^{210}Pb observed.

In intermediate and deep waters, total activities of ^{210}Pb and ^{210}Po increased to 4.3 ± 1.7 dpm 100L^{-1} (n = 65) and 3.4 ± 1.6 dpm 100L^{-1} (n = 64), respectively. These activities, in the case of ^{210}Pb, were mostly lower than those found in the mixed layer, but, in the case of ^{210}Po, they were generally higher than in overlying waters (Figure 3).

Over the Alpha Ridge, good agreement was found between the activities measured at stations 338 and 342 at 1000 m, which averaged 5.0 ± 1.1 dpm 100L^{-1} for ^{210}Pb and 4.06 ± 0.09 dpm 100L^{-1} for ^{210}Po, and those found at the CESAR site at the same depth (3.9 ± 0.2 dpm 100L^{-1} and 4.3 ± 0.2 dpm 100L^{-1}, respectively; Moore and Smith, 1986). In the Eurasian Basin, the ^{210}Pb and ^{210}Po activities measured in the present study at 300 m were, on average, 5.6 ± 0.6 dpm 100L^{-1} and 3.9 ± 0.3 dpm 100L^{-1}, respectively, in the Nansen Basin (stations 255 and 260), and 2.49 ± 0.11 dpm 100L^{-1} and 2.43 ± 0.12 dpm 100L^{-1}, respectively, in the Amundsen Basin (station 309). These activities are also comparable to those measured in the same basins and water depth in summer 2012 (Roca-Martí et al., 2016). Based on the inspection of temperature-salinity properties in summer 2007 (not shown), Atlantic Water seems to originate in the Barents Sea inflow branch at station 309, the Fram Strait branch at station 255 or a mixture of the two at station 260. Therefore, besides removal during transit, enhanced particle scavenging in the Barents Sea could also help explain the lower activities of both radionuclides in the Amundsen Basin with

respect to those measured at stations affected by the Fram Strait branch, similar to the interpretation by Smith et al. (2003) for the lower halocline.

Regarding the total $^{210}Po/^{210}Pb$ ratios, significant deficits of ^{210}Po (i.e. ratio <0.90, considering uncertainties) were observed throughout most of the water column in the study area. The most substantial deficits of ^{210}Po were found in surface and subsurface waters spanning depths from 10 to 200 m (Figures 2 and 4), covering the mixed layer and the halocline(s): total $^{210}Po/^{210}Pb$ ratios averaged 0.46 ± 0.19 in the mixed layer (n = 38), 0.46 ± 0.14 in the upper halocline (n = 7) and 0.6 ± 0.3 in the lower halocline (n = 17). Po-210 deficits in the upper water column are usually attributed to biological particle production and subsequent scavenging and export, which will be discussed in Section 3.3.

In the upper 25 m, we find good agreement between the mean total $^{210}Po/^{210}Pb$ ratio in summer 2007 (0.5 ± 0.2, n = 14; including all profiles except stations 237, 276 and 411 for lack of data) and that measured in the Eurasian Basin in summer 2012 (0.66 ± 0.19, n = 7; Roca-Martí et al., 2016). These results are also consistent with those obtained at single depths (10-20 m) from the Chukchi Sea to the Mendeleev Ridge in summer 1994 (0.6 ± 0.3, n = 6; Smith et al., 2003). Total $^{210}Po/^{210}Pb$ ratios of 0.50 to 0.60 correspond to a ^{210}Po residence time of 7 to 10 months based on a steady-state balance and the assumption of negligible atmospheric flux of ^{210}Po (Nozaki et al., 1998). Although the rather low biological productivity of the Arctic ice-covered waters, this estimate compares well with the residence time obtained for the mixed layer in the Atlantic, Pacific and Indian Oceans (~7 months; Bacon et al., 1976; Cochran et al., 1983; Nozaki et al., 1976; Shannon et al., 1970). Similarly, the mean total $^{210}Po/^{210}Pb$ ratio in the upper 200 m was 0.6 ± 0.3 (n = 12; including all profiles except stations 260, 266, 276, 407 and 411 for lack of data). This result is lower than that found in summer 2012 (0.9 ± 0.6, n = 7; Roca-Martí et al., 2016) and at the CESAR site in spring 1983 (0.96 ± 0.04, n = 1; Moore and Smith, 1986).

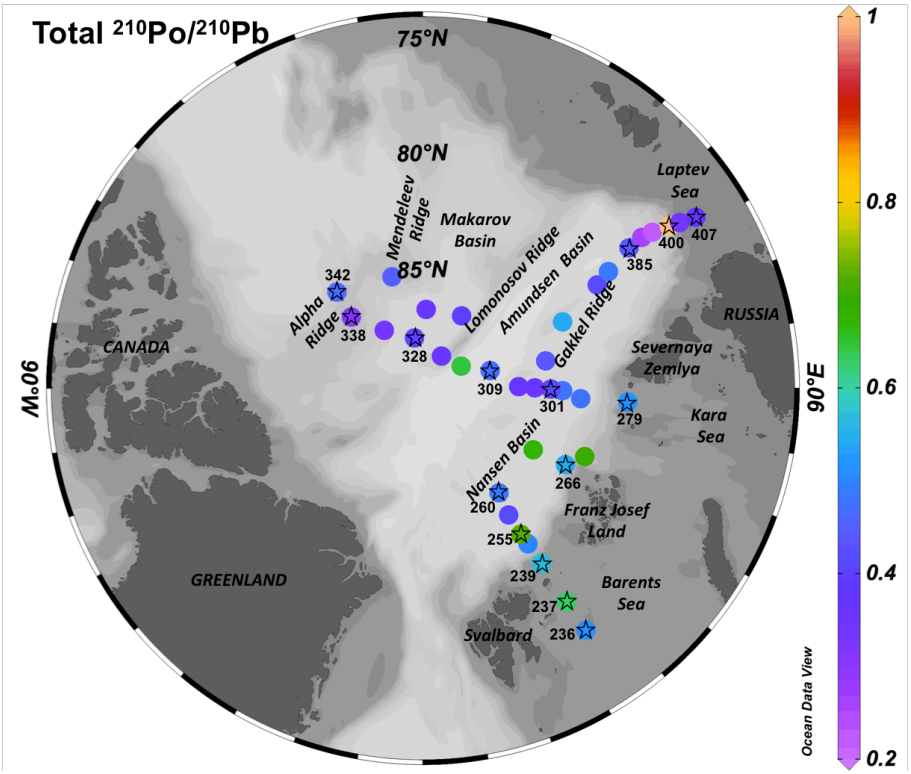

Figure 4: Total $^{210}Po/^{210}Pb$ activity ratios in surface waters (10 m). Stars indicate the stations sampled for vertical profiles (station numbers shown).

Apart from the ^{210}Po deficits found in the upper ocean, they were also detected in the mesopelagic and bathypelagic zones. Total $^{210}Po/^{210}Pb$ ratios averaged 0.8 ± 0.5 in intermediate and deep waters (n = 64), where equilibrium between both radionuclides was only approached in one-third of the instances (ratio >0.90, Table S1, Supplemental Material). The magnitude of these ^{210}Po deficits at depth could indicate that they do not solely reflect the settling of particles to the deep ocean. Considering the previous literature, mean total $^{210}Po/^{210}Pb$ ratios were near equilibrium in the Eurasian Basin (1.0 ± 0.5, n = 14, depth range: 300-400 m; Roca-Martí et al., 2016) and at the CESAR site (0.9 ± 0.2, n = 3, depth range: 800-1200 m; Moore and Smith, 1986), but were significantly far from equilibrium during the Arctic Ocean Section (0.6 ± 0.4, n = 17, depth range: 300-4200 m; Smith et al., 2003) that went from the Chukchi Sea to the Fram Strait (Figure S2). A deficiency of ^{210}Po in the ocean interior has also been observed in other oceanic regions (e.g. Kim and Church, 2001; Nozaki et al., 1997, 1990; Sarin et al., 1994; Thomson and Turekian, 1976), but its origin is still unclear. Hence, while this study cannot elucidate the reasons for these deficits, the interpretation of the $^{210}Po/^{210}Pb$ pair at depth remains uncertain until further investigations are made.

3.1.2. Particulate $^{210}Po/^{210}Pb$ ratios

Particulate ^{210}Pb and ^{210}Po activities can be found in the Supplemental Material.

Particulate $^{210}Po/^{210}Pb$ ratios averaged 0.5 ± 0.5 in the mixed layer (n = 38), 0.30 ± 0.18 in the upper halocline (n = 7), 0.5 ± 0.3 in the lower halocline (n = 19), and 0.8 ± 0.5 in intermediate waters down to 500 m (n = 28). Only 15% of the samples showed ^{210}Po enrichment (i.e. particulate $^{210}Po/^{210}Pb$ ratio >1.10), which were mainly located in the Nansen Basin (up to 4-8 at 10-25 m; Figure 5) around the area where large deficits of ^{210}Po were found (see Section 3.3). The two studies that have previously reported particulate ^{210}Pb and ^{210}Po activities in the Arctic Ocean have also presented $^{210}Po/^{210}Pb$ ratios lower than 1 for particles ≥0.45 μm (Moore and Smith, 1986) and ≥53 μm (Roca-Martí et al., 2016) at depths from 25 to 800 m over the Alpha Ridge and the Eurasian Basin. The overall low ratios obtained seem to be inconsistent with the preferential removal of ^{210}Po by particle export shown by the widespread deficiency of ^{210}Po in the upper ocean in summer 2007 (see Sections 3.1.1 and 3.3).

The particles we analysed (≥1 μm) were obtained from 40-160 L of seawater collected with Niskin bottles, which would basically represent the suspended (or small) particle fraction (Bishop et al., 2012). Indeed, the quantification of ^{210}Pb and ^{210}Po in large particles (>53-70 μm), those that contribute most to particle fluxes (see references in Lam and Marchal, 2015), requires filtration of large volumes, particularly in the central Arctic (several hundreds of liters may not be enough, Roca-Martí et al., 2016). Therefore, we believe that the particulate activities presented here correspond to small, suspended particles rather than rare, large, sinking particles. Yet, these particle pools could have a similar composition by aggregation and disaggregation. Previous studies have shown that the degree of this particle exchange can vary geographically and seasonally in relation to the dominant particle type and plankton community structure (Abramson et al., 2010; Lam and Marchal, 2015). While we do not know to what extent the collected particles would represent the large particles in late summer, particulate $^{210}Po/^{210}Pb$ ratios <1 indicate that these particles would not represent the sinking particle pool that created the ^{210}Po deficiency in seawater. Hence, these observations suggest that: (i) large particles in the late summer are not well represented in this study, and/or (ii) ^{210}Po export mostly occurred earlier in the season and particle composition changed during spring/summer.

This latter possibility is consistent with the conclusions drawn by Roca-Martí et al. (2016).

Particle types that could be found during the Arctic late summer that could help explain the measured particulate $^{210}Po/^{210}Pb$ ratios <1 include: sea-ice drafted particles enriched in ^{210}Pb via atmospheric input ($^{210}Po/^{210}Pb$ ratios <1 in sea-ice sediments; Roca-Martí et al., 2016), material remineralized by chemical and biological processes (Stewart et al., 2007b), faecal pellets (Rodriguez y Baena et al., 2007; Stewart et al., 2005), picoplankton aggregates (Stewart et al., 2010) and substrates rich in transparent exopolymer particles (Quigley et al., 2002). Also, low particulate $^{210}Po/^{210}Pb$ ratios (≤1) in shelf waters could be due to the presence of terrestrial and riverine particles (Nozaki et al., 1998; Tateda et al., 2003). Sampling of size-fractionated particles, ideally at different times during the growing season, coupled with particle composition analyses should be carried out in future works to infer what controls the particulate $^{210}Po/^{210}Pb$ ratios in the Arctic and, specifically, those lower than 1.

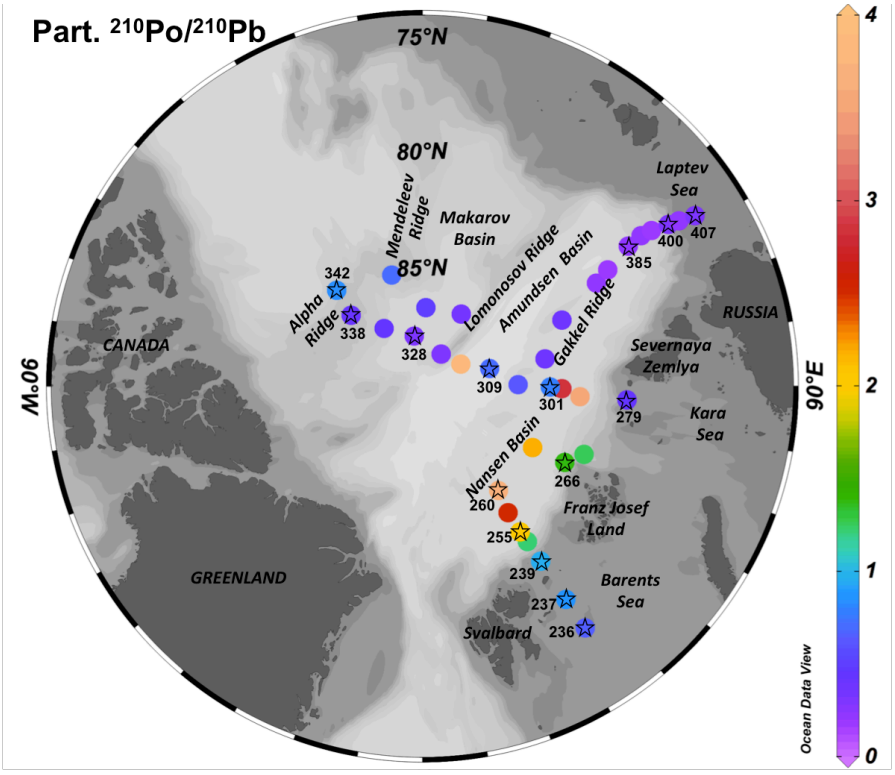

Figure 5: Particulate $^{210}Po/^{210}Pb$ activity ratios in surface waters (10 m). Stars indicate the stations sampled for vertical profiles (station numbers shown).

3.2. Annual new primary production

The annual new primary production estimates in the Nansen, Amundsen and Makarov Basins are presented in Table 2. The nitrogen consumed above the winter mixed layer depth during the productive season was on average 90 ± 40 mmol m^{-2} in the Eurasian sector (stations 255, 260, 266, 301, 309 and 385), whereas it was 250 ± 90 mmol m^{-2} in the Canadian sector (stations 328, 338 and 342). Annual nitrogen-derived primary production estimates were similar across the Nansen and Amundsen Basins, with an average of 7 ± 3 g C m^{-2} yr^{-1}, although it was about four times lower north of Franz Josef Land (station 266). In the Makarov Basin, annual new primary production was always higher than in the Eurasian Basin, averaging 20 ± 7 g C m^{-2} yr^{-1}. Phosphate-derived estimates were similar to those derived from nitrogen (<6% difference) at most of the stations. Ulfsbo et al. (2014) also found higher estimates in the Makarov Basin, particularly over the Mendeleev Ridge, when compared to the other basins. Globally, the annual new primary production was on average 12 g C m^{-2} yr^{-1} considering all the nitrogen- and phosphate-derived estimates, which is similar to reported estimates of about 9 g C m^{-2} yr^{-1} including values from the Nansen, Amundsen, Makarov and Canada Basins during years 2011 and 2012 (Fernández-Méndez et al., 2015; Ulfsbo et al., 2014).

Silicate-derived new primary production estimates were on average 2.3 ± 1.9 g C m^{-2} yr^{-1} in the Eurasian sector, whereas they averaged 32 ± 17 g C m^{-2} yr^{-1} in the Makarov Basin. Comparison between silicate-derived new primary production with the other two estimates gives an indication of the contribution of diatoms to new production. Diatom production estimates varied widely across the study area, amounting between 10 to 70% of annual new primary production in the Eurasian sector and about 100% in the Makarov Basin. This suggests that diatom production had an important role in the Canadian sector of the study area during the productive season in 2007. Yet, we note that the higher silicate-derivate new primary production estimates obtained in the Makarov Basin compared to those from nitrogen and phosphate indicate that the former estimates may be overestimated. This bias can be due to the advected silicate maximum in the upper halocline and uncertainties in determining silicate concentrations in the winter mixed layer, together with the variability in N/Si ratios reported for Arctic diatoms (Fernández-Méndez et al., 2015). Therefore, silicate-derived new primary production estimates in the Makarov Basin should be taken with caution.

Table 2: Nitrite+nitrate, phosphate and silicate drawdown above the winter mixed layer depth (WMLD) and annual new primary production estimated using the Redfield-Brzezinski ratio (106C:16N:15Si:1P).

Station	WMLD (m)	Nutrient deficits (mmol m^{-2})			Annual new production (g C m^{-2} yr^{-1})		
		Nitrite+nitrate	Phosphate	Silicate	Nitrite+nitrate	Phosphate	Silicate
255	38	86	5.0	52	6.8	6.4	4.4
260[a]	81	88	4.9	17	7.0	6.2	1.5
266	22	26	1.6	11	2.0	2.0	0.91
301	60	120	7.3	15	9.8	9.3	1.3
309	59	130	8.4	59	10	11	5.0
328	54	190	16	210	15	21	18
338	60	210	13	310	17	17	27
342	67	350	30	590	28	38	50
385[a]	50	88	5.9	10	7.0	7.6	0.86

[a] Different casts were taken for nutrient deficits and WMLD determination.

3.3. Particle export in the Arctic as revealed by ^{210}Po deficits

On the Arctic shelves visited in late summer 2007, Cai et al. (2010) found ^{234}Th deficits in the upper 100 m of the water column in association with enhanced Chl-a concentrations, indicating that in situ production and export of biogenic particles were the main mechanism for ^{234}Th removal. Nevertheless, we did not observe significant correlations between Chl-a concentrations and ^{210}Po deficits (not shown). This may not be surprising given that Chl-a concentration is a snapshot of the sampling time (i.e. late summer), whereas ^{210}Po integrates a time scale of several months, covering, in this case, from the onset of the growing season, which occurs as early as March (Wassmann and Reigstad, 2011). Satellite images of the ice-free area in the Barents Sea revealed five-fold higher Chl-a concentrations in May-June with respect to those in July-August in 2007, showing that the sampling was conducted in a post-bloom situation (Klunder et al., 2012). Indeed, the concentrations of nutrients in the mixed layer were low during the expedition (see details in Supplemental Material).

Seasonal estimates of primary production can be helpful to obtain a wider perspective on production of organic matter than that at the time of sampling. However, the method used here to estimate annual new primary production does not allow obtaining reliable results in the shelf environment, where the advective input of nutrients could significantly bias the estimates. Therefore, we cannot provide evidence of the relation between ^{210}Po deficits and annual new primary production (and subsequent export) in the Barents, Kara and Laptev Seas.

As described in Section 3.1.1, ^{210}Po deficits were not restricted to the shelf environment, but they were also pronounced in the central Arctic, without showing any gradient from

504 the shelves to the central Arctic (Figures 2 and 4). During the expedition, the basins were
505 characterized by generally low Chl-a levels and very low particle export, as reported by
506 Cai et al. (2010) using ^{234}Th. This apparent discrepancy between ^{234}Th and ^{210}Po may be
507 explained by significant export fluxes that occurred more than one month before
508 sampling, which would be recorded by ^{210}Po but missed by ^{234}Th. In this line, Rutgers
509 van der Loeff et al. (2012) argued that the ^{234}Th-based scavenging rate could not explain
510 the distribution of ^{228}Th in the central Arctic in summer 2007 due to seasonal variations
511 in scavenging and the different half-lives of ^{234}Th and ^{228}Th. In the following discussion,
512 we explore whether the results of ^{210}Po and ^{234}Th indicate a seasonal variation in particle
513 export by comparing the deficits of ^{210}Po with the estimates of annual new primary
514 production obtained from the Nansen, Amundsen and Makarov Basins.

515 Although the number of data points is small, we find a negative relationship between
516 annual new primary production estimates based on nitrogen consumption and total
517 ^{210}Po/^{210}Pb ratios in the upper 25 and 200 m of the basin stations ($p < 0.05$ for each depth;
518 25 m: Spearman correlation coefficient, $\rho = -0.72$, $n = 9$; 200 m: $\rho = -0.79$, $n = 7$; Figure
519 6). This suggests that greater deficits of ^{210}Po in the upper water column of the Arctic
520 were related to higher in situ new production and subsequent export of biogenic material
521 to depth. This would be analogous to the situation reported for the Eurasian Basin in 2012,
522 based on ^{210}Po/^{210}Pb and nutrient sampling also conducted during the late summer (from
523 11 August to 22 September; Roca-Martí et al., 2016). Indeed, if we combine the results
524 from both studies, the significance of the observed relationship increases ($p < 0.01$ for
525 each depth; 25 m: Spearman correlation coefficient, $\rho = -0.73$, $n = 16$; 200 m: $\rho = -0.68$,
526 $n = 14$; Figure 6). This shows the potential use of the ^{210}Po/^{210}Pb proxy as an indicator of
527 annual new primary production in the central Arctic, although futher investigations will
528 be necessary.

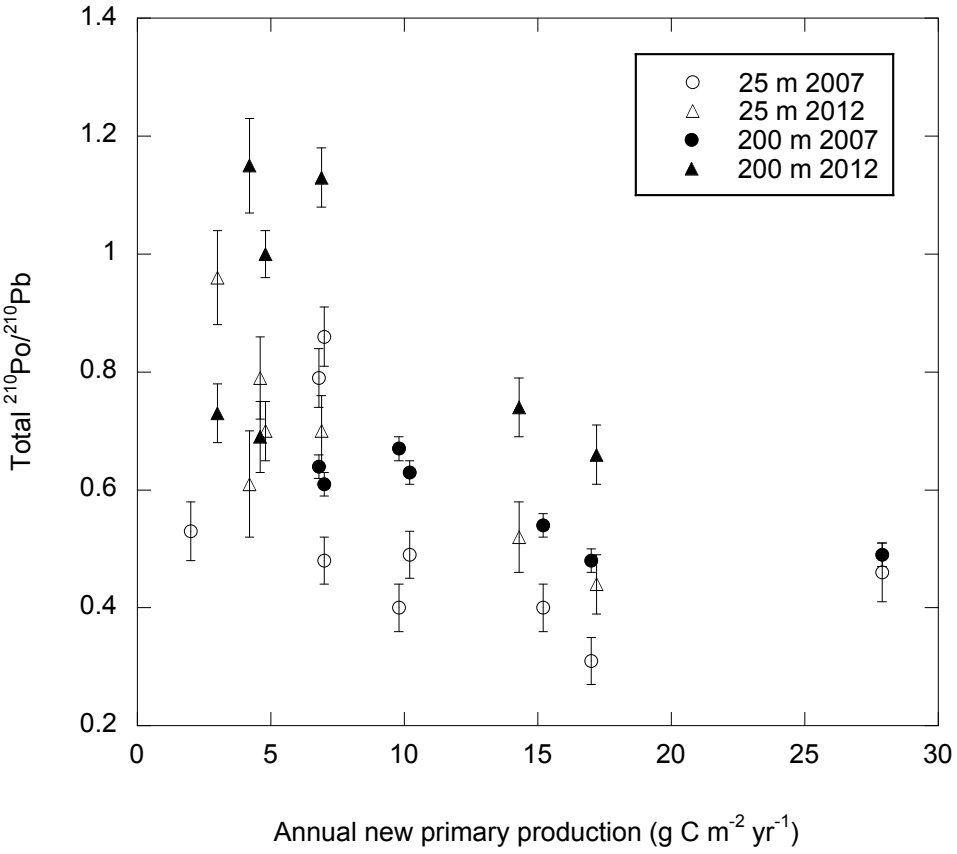

529

530 **Figure 6** Total $^{210}Po/^{210}Pb$ activity ratios in the upper 25 m (white) and 200 m (black) vs nitrogen-derived
531 new primary production estimates that encompass the Arctic growing season in summers 2007 (circles; this
532 study) and 2012 (triangles; Roca-Martí et al., 2016).

533 Total $^{210}Po/^{210}Pb$ ratios were lower for waters in the salinity range from about 27 to 34,
534 covering the mixed layer and the upper halocline (basically confined in the Canadian
535 sector), than for higher salinities and, hence, deeper waters. The lower salinity waters
536 were influenced by Pacific Water or freshwater inputs from river runoff and local
537 precipitation (jointly referred to as river water) and net sea-ice melting (see details in
538 Bauch et al., 2011; Roeske et al., 2012; Rutgers van der Loeff et al., 2012). The
539 contribution of these water sources to surface and subsurface waters is discussed below
540 in relation to the total $^{210}Po/^{210}Pb$ ratios measured in each area in order to investigate the
541 processes that drove the ^{210}Po deficits in 2007.

542 In the Makarov Basin, $^{210}Po/^{210}Pb$ ratios were especially low with values generally <0.50
543 for waters extending down to the upper halocline. Over the Alpha Ridge, sea-ice
544 meltwater amounted to 1 to 2% of surface waters at stations 338 and 342 (Bauch et al.,
545 2011; Rutgers van der Loeff et al., 2012). Roca-Martí et al. (2016) showed that a complete
546 melting of sea ice in the central Arctic would change the total $^{210}Po/^{210}Pb$ ratios by less

than 10% in surface waters. Therefore, the substantial deficits of ^{210}Po observed would not be explained by the input of sea-ice meltwater depleted in ^{210}Po with respect to ^{210}Pb. On the other hand, the upper 100 m of stations 328, 338 and 342 were composed of 5 to 15% of river water and a large fraction of Pacific Water (up to >80%; Bauch et al., 2011). Seawater with salinities of ~30 to 32 (part of the Polar Mixed Layer) found in the central Arctic, especially near the Lomonosov Ridge (stations 320 and 328), originated from the bottom of the Laptev Sea (Bauch et al., 2011), whereas waters with salinities of 32.5 to 33.3 (part of the upper halocline) found over the Alpha and Mendeleev Ridges came from the Chukchi Sea (Roeske et al., 2012). These waters from the Laptev and Chukchi Seas carried river and Pacific-derived water, respectively, and were transported to the central Arctic by the Transpolar Drift. Thus, a hypothesis would be that the deficiency of ^{210}Po observed in the upper water column of the Makarov Basin was created in the shelf regime as a consequence of biological activity and particle export. This possibility would be consistent with a transit time of less than three months, comparing the most substantial deficits of ^{210}Po that occurred near the continental margin to the deficits measured over the Alpha Ridge (^{210}Po/^{210}Pb ratios of ~0.2 vs. ~0.4, respectively). However, it was estimated that the shelf waters encountered at the surface of the Makarov Basin and the Lomonosov Ridge in summer 2007 travelled for at least seven months (Rutgers van der Loeff et al., 2018).

Another possibility could be that ^{210}Po deficits in the Makarov Basin originated in situ. During the productive season in 2007, the average annual new primary production in the Makarov Basin was higher than in the Eurasian Basin by a factor of 3, and diatoms appeared to dominate the phytoplankton community (see Section 3.2). Consistent with this, Middag et al. (2009) measured minimum concentrations of aluminium in the upper 300 m of the Makarov Basin during the same expedition, which were related to biological uptake favoured by silica inputs from the upper halocline. Particularly, at stations 338 and 342, nitrate was depleted from the surface to 50 m depth. The mixed layer depth at these stations decreased from 60-67 m in winter to 20-26 m at the sampling time and, therefore, the uptake of nitrate had to take place early in the productive season when the seasonal mixed layer was deep enough. This would most likely have occurred before July, since from May surface warming and sea-ice melt establish stratification and, thus, limit the mixing of nutrients within the winter mixed layer (Kawaguchi et al., 2012; Korhonen et al., 2013). Therefore, the ^{210}Po deficiency found in the Makarov Basin likely originated

580 in situ by means of enhanced new primary production and subsequent export. Over the
581 Alpha Ridge, in particular, this might have been related to ice-algae export resulting from
582 sea-ice melt, as observed in the Eurasian Basin during the record sea-ice minimum in
583 2012. In that year, a widespread deposition of sea-ice diatom aggregates was observed on
584 the seafloor (>3000 m, Boetius et al., 2013) and the largest deposits were found together
585 with the strongest depletion of ^{210}Po in seawater (Roca-Martí et al., 2016).

586 In the Barents Sea and Nansen Basin, the major deficits of ^{210}Po (total ^{210}Po/^{210}Pb ratios
587 ≤0.50) were found in cold and relatively low salinity waters in the upper 75 m of section
588 1 (stations 236, 237, 249, 255, 257 and 260). Most of this section had a significant fraction
589 of sea-ice meltwater in the upper 50 to 100 m (~2%; Bauch et al., 2011). Substantial
590 depletions of ^{234}Th, ^{226}Ra, Ba and dissolved Fe were concurrent with the ice edge (81-
591 82ºN), together with particularly high phytoplankton biomass, suggesting the occurrence
592 of an ice-edge bloom (Cai et al., 2010; Klunder et al., 2012; Roeske et al., 2012; Rutgers
593 van der Loeff et al., 2012). As observed for ^{210}Po, ^{234}Th was depleted in the upper 100 m
594 south of the ice edge (Cai et al., 2010), where Chl-a levels were found to be very high
595 two months prior to the sampling (~5 mg m^{-3}; Klunder et al., 2012). In the nutrient-rich
596 Barents Sea, the association between freshwater from sea-ice melt and ^{210}Po deficits may
597 be explained by enhanced primary production when melting occurs. This would improve
598 light conditions for phytoplankton growth and subsequent particle settling, in accordance
599 with previous studies of particle fluxes conducted in the area (Coppola et al., 2002;
600 Lalande et al., 2008; Wassmann et al., 2004; Wiedmann et al., 2014).

601 In the Laptev section, river water had an important presence in the entire water column
602 of the Laptev Sea and in the upper 25 m offshore (Bauch et al., 2011). The inflow of
603 waters from the Lena River supplies significant amounts of nutrients to the Laptev Sea
604 (e.g. Le Fouest et al., 2013), which may have nourished the high phytoplankton biomass
605 observed on the shelf (Cai et al., 2010). Moreover, a large reduction of the sea-ice cover
606 was observed in the Laptev sector in summer 2007 compared to earlier years (Comiso et
607 al., 2008), and sea-ice meltwater in surface waters was detected from the shelf to station
608 385 (Bauch et al., 2011). This sea-ice decline extended the growing season by 50 to 80
609 days and boosted primary production (Arrigo et al., 2008). The maximum inventory of
610 Chl-a was measured at station 407 (Cai et al., 2010), where a substantial deficit of ^{210}Po
611 was found in surface waters overlying an excess at 25 m (total ^{210}Po/^{210}Pb ratios of 0.37

612 and 2.8, respectively). This suggests export driven by biogenic particles in surface waters
613 and remineralization or particle disaggregation below, in agreement with the conclusions
614 drawn from Ba, ^{226}Ra and dissolved Fe in the Laptev Sea (Klunder et al., 2012; Roeske
615 et al., 2012; Rutgers van der Loeff et al., 2012). The ^{210}Po deficits found north of the
616 Laptev Sea (stations 371-400) could be related to biogenic fluxes that occurred prior to
617 sampling, as they are significant in this area from June to August (Fahl and Nöthig, 2007;
618 Lalande et al., 2009b). Indeed, sediment traps deployed on the Laptev slope revealed
619 about two-fold higher annual POC export in 2006-2007 relative to 2005-2006 (Lalande
620 et al., 2009a). This was mainly attributed to an increase in POC export during and
621 following sea-ice melt in 2007, with maximum fluxes in July.

622 **4. Conclusions**

623 We investigated the distribution of ^{210}Pb and ^{210}Po in the water column of various seas
624 (Barents, Kara and Laptev) and basins (Nansen, Amundsen and Makarov) of the Arctic
625 Ocean in summer 2007. Total activities of ^{210}Pb and ^{210}Po were minimum in the upper
626 and lower haloclines, especially in the Makarov and eastern Eurasian Basins, at
627 approximately 60-130 m. This is partly ascribed to particle scavenging on the shelves
628 where these water masses are formed, boundary current transport and subsequent
629 transport into the central Arctic.

630 During the sea-ice minimum in 2007, widespread deficits of ^{210}Po in the upper water
631 column were observed all over the Arctic, both on the shelves and in the basins. In the
632 shelf areas of the Barents and Laptev Seas, ^{210}Po deficits were related to elevated
633 phytoplankton biomass and particle export. These deficits were usually associated with
634 sea-ice meltwater and riverine water inputs, which may improve light and/or nutrient
635 conditions for photosynthesis. In the basins, estimates of annual new primary production
636 were negatively correlated to total ^{210}Po/^{210}Pb ratios in the upper 200 m of the water
637 column, suggesting that in situ production and subsequent export controlled the removal
638 of ^{210}Po also in this environment. This shows the potential use of the ^{210}Po/^{210}Pb proxy as
639 an indicator of annual new primary production in the central Arctic, although more data
640 will be necessary. The ^{210}Po deficits were most substantial (total ^{210}Po/^{210}Pb ratios <0.50)
641 in the mixed layer and the upper halocline of the Makarov Basin, where estimates of
642 annual new primary production were found to be particularly high.

643 Unlike ^{210}Po, ^{234}Th deficits were very small and not significant below 25 m over the
644 basins in August-September 2007 (Cai et al., 2010). Given the shorter half-life of ^{234}Th,
645 this indicates that particle export fluxes in the Arctic basins would have been higher
646 before July-August than later in the summer, in line with the conclusions drawn by Roca-
647 Martí et al. (2016) during the record sea-ice minimum in 2012.

648 Deficits of total ^{210}Po in intermediate and deep waters (approx. 200-3000 m) were
649 frequently observed, as well as particulate ^{210}Po/^{210}Pb ratios below 1, although the reasons
650 are not clear. Sampling of size-fractionated particles in various periods of the growing
651 season together with analyses of particle composition shall be helpful to better understand
652 the biogeochemical behaviour of these radionuclides.

653 Acknowledgements

654 We would like to thank the crew of the R/V Polarstern and the scientists on board for
655 their cooperation during the ARK-XXII/2 expedition. We greatly appreciate the hard
656 work of Oliver Lechtenfeld who collected and processed the samples on board. Thanks
657 to Dorothea Bauch for sharing her results on freshwater origin and Adam Ulfsbo for
658 providing insightful comments on the estimates of primary production. This project was
659 partly supported by the Ministerio de Ciencia e Innovación (CTM2011-28452, Spain).
660 We wish to acknowledge the support of the Generalitat de Catalunya to the research group
661 MERS (2017 SGR-1588). This work is contributing to the ICTA 'Unit of Excellence'
662 (MinECo, MDM2015-0552). M.R.-M. was supported by a Spanish PhD fellowship
663 (AP2010-2510) and an Australian postdoctoral fellowship (2017 Endeavour Research
664 Fellowship).

665 Abramson, L., Lee, C., Liu, Z., Wakeham, S.G., Szlosek, J., 2010. Exchange between
666 suspended and sinking particles in the northwest Mediterranean as inferred from
667 the organic composition of in situ pump and sediment trap samples. Limnol.
668 Oceanogr. 55, 725–739. doi:10.4319/lo.2010.55.2.0725

669 Ardyna, M., Babin, M., Gosselin, M., Devred, E., Rainville, L., Tremblay, J.-É., 2014.
670 Recent Arctic Ocean sea ice loss triggers novel fall phytoplankton blooms.
671 Geophys. Res. Lett. 41, 6207–6212. doi:10.1002/2014GL061047

672 Arrigo, K.R., van Dijken, G., Pabi, S., 2008. Impact of a shrinking Arctic ice cover on
673 marine primary production. Geophys. Res. Lett. 35, L19603.

674 Arrigo, K.R., van Dijken, G.L., 2015. Continued increases in Arctic Ocean primary
675 production. Prog. Oceanogr. 136, 60–70. doi:10.1016/j.pocean.2015.05.002

676 Bacon, M.P., Belastock, R.A., Tecotzky, M., Turekian, K.K., Spencer, D.W., 1988.
677 Lead-210 and polonium-210 in ocean water profiles of the continental shelf and
678 slope south of New England. Cont. Shelf Res. 8, 841–853. doi:10.1016/0278-
679 4343(88)90079-9

680 Bacon, M.P., Spencer, D.W., Brewer, P.G., 1976. $^{210}Pb/^{226}Ra$ and $^{210}Po/^{210}Pb$
681 disequilibria in seawater and suspended particulate matter. Earth Planet. Sci. Lett.
682 32, 277–296. doi:10.1016/0012-821X(76)90068-6

683 Baskaran, M., 2011. Po-210 and Pb-210 as atmospheric tracers and global atmospheric
684 Pb-210 fallout: a review. J. Environ. Radioact. 102, 500–513.
685 doi:10.1016/j.jenvrad.2010.10.007

686 Baskaran, M., Swarzenski, P.W., Porcelli, D., 2003. Role of colloidal material in the
687 removal of ^{234}Th in the Canada basin of the Arctic Ocean. Deep Sea Res. Part I
688 Oceanogr. Res. Pap. 50, 1353–1373. doi:10.1016/S0967-0637(03)00140-7

689 Bauch, D., Hölemann, J., Willmes, S., Gröger, M., Novikhin, A., Nikulina, A., Kassens,
690 H., Timokhov, L., 2010. Changes in distribution of brine waters on the Laptev Sea
691 shelf in 2007. J. Geophys. Res. 115, C11008. doi:10.1029/2010JC006249

692 Bauch, D., Rutgers van der Loeff, M., Andersen, N., Torres-Valdes, S., Bakker, K.,
693 Abrahamsen, E.P., 2011. Origin of freshwater and polynya water in the Arctic
694 Ocean halocline in summer 2007. Prog. Oceanogr. 91, 482–495.
695 doi:10.1016/j.pocean.2011.07.017

696 Bishop, J.K.B., Lam, P.J., Wood, T.J., 2012. Getting good particles: Accurate sampling
697 of particles by large volume in-situ filtration. Limnol. Oceanogr. Methods 10, 681–
698 710. doi:10.4319/lom.2012.10.681

699 Boetius, A., Albrecht, S., Bakker, K., Bienhold, C., Felden, J., Fernández-Méndez, M.,
700 Hendricks, S., Katlein, C., Lalande, C., Krumpen, T., Nicolaus, M., Peeken, I.,
701 Rabe, B., Rogacheva, A., Rybakova, E., Somavilla, R., Wenzhöfer, F., RV
702 Polarstern ARK27-3-Shipboard Science Party, 2013. Export of algal biomass from
703 the melting Arctic sea ice. Science 339, 1430–1432. doi:10.1126/science.1231346

704 Brzezinski, M.A., 1985. The Si:C:N ratio of marine diatoms: interspecific variability

and the effect of some environmental variables. J. Phycol. 21, 347–357. doi:10.1111/j.0022-3646.1985.00347.x

Cai, P., Rutgers van der Loeff, M.M., Stimac, I., Nöthig, E.-M., Lepore, K., Moran, S.B., 2010. Low export flux of particulate organic carbon in the central Arctic Ocean as revealed by ^{234}Th:^{238}U disequilibrium. J. Geophys. Res. 115, C10037. doi:10.1029/2009JC005595

Cámara-Mor, P., Masqué, P., Garcia-Orellana, J., Kern, S., Cochran, J.K., Hanfland, C., 2011. Interception of atmospheric fluxes by Arctic sea ice: Evidence from cosmogenic ^{7}Be. J. Geophys. Res. Ocean. 116, C12041. doi:10.1029/2010JC006847

Cauwet, G., Sidorov, I., 1996. The biogeochemistry of Lena River: organic carbon and nutrients distribution. Mar. Chem. 53, 211–227. doi:10.1016/0304-4203(95)00090-9

Chen, M., Ma, Q., Guo, L., Qiu, Y., Li, Y., Yang, W., 2012. Importance of lateral transport processes to ^{210}Pb budget in the eastern Chukchi Sea during summer 2003. Deep Sea Res. Part II Top. Stud. Oceanogr. 81–84, 53–62. doi:10.1016/j.dsr2.2012.03.011

Cherrier, J., Burnett, W.C., LaRock, P.A., 1995. Uptake of polonium and sulfur by bacteria. Geomicrobiol. J. 13, 103–115. doi:10.1080/01490459509378009

Church, T., Rigaud, S., Baskaran, M., Kumar, A., Friedrich, J., Masqué, P., Puigcorbé, V., Kim, G., Radakovitch, O., Hong, G., Choi, H., Stewart, G., 2012. Intercalibration studies of ^{210}Po and ^{210}Pb in dissolved and particulate seawater samples. Limnol. Oceanogr. Methods 10, 776–789.

Cochran, J.K., Bacon, M.P., Krishnaswami, S., Turekian, K.K., 1983. ^{210}Po and ^{210}Pb distributions in the central and eastern Indian Ocean. Earth Planet. Sci. Lett. 65, 433–452. doi:10.1016/0012-821X(83)90180-2

Cochran, J.K., Masqué, P., 2003. Short-lived U/Th Series Radionuclides in the Ocean: Tracers for Scavenging Rates, Export Fluxes and Particle Dynamics. Rev. Mineral. Geochemistry 52, 461–492. doi:10.2113/0520461

Codispoti, L.A., Kelly, V., Thessen, A., Matrai, P., Suttles, S., Hill, V., Steele, M., Light, B., 2013. Synthesis of primary production in the Arctic Ocean: III. Nitrate and phosphate based estimates of net community production. Prog. Oceanogr. 110, 126–150. doi:10.1016/j.pocean.2012.11.006

Comiso, J.C., Parkinson, C.L., Gersten, R., Stock, L., 2008. Accelerated decline in the Arctic sea ice cover. Geophys. Res. Lett. 35, L01703. doi:10.1029/2007GL031972

Coppola, L., Roy-Barman, M., Wassmann, P., Mulsow, S., Jeandel, C., 2002. Calibration of sediment traps and particulate organic carbon export using ^{234}Th in the Barents Sea. Mar. Chem. 80, 11–26. doi:10.1016/S0304-4203(02)00071-3

Eicken, H., Reimnitz, E., Alexandrov, V., Martin, T., Kassens, H., Viehoff, T., 1997. Sea-ice processes in the Laptev Sea and their importance for sediment export.

745 Cont. Shelf Res. 17, 205–233. doi:10.1016/S0278-4343(96)00024-6

746 Ekwurzel, B., Schlosser, P., Mortlock, R.A., Fairbanks, R.G., Swift, J.H., 2001. River
747 runoff, sea ice meltwater, and Pacific water distribution and mean residence times
748 in the Arctic Ocean. J. Geophys. Res. Ocean. 106, 9075–9092.
749 doi:10.1029/1999JC000024

750 Fahl, K., Nöthig, E.-M., 2007. Lithogenic and biogenic particle fluxes on the
751 Lomonosov Ridge (central Arctic Ocean) and their relevance for sediment
752 accumulation: Vertical vs. lateral transport. Deep Sea Res. Part I Oceanogr. Res.
753 Pap. 54, 1256–1272. doi:10.1016/j.dsr.2007.04.014

754 Fernández-Méndez, M., Katlein, C., Rabe, B., Nicolaus, M., Peeken, I., Bakker, K.,
755 Flores, H., Boetius, A., 2015. Photosynthetic production in the central Arctic
756 Ocean during the record sea-ice minimum in 2012. Biogeosciences 12, 3525–3549.
757 doi:10.5194/bg-12-3525-2015

758 Findlay, H.S., Gibson, G., Kedra, M., Morata, N., Orchowska, M., Pavlov, A.K.,
759 Reigstad, M., Silyakova, A., Tremblay, J.É., Walczowski, W., Weydmann, A.,
760 Logvinova, C., 2015. Responses in Arctic marine carbon cycle processes:
761 Conceptual scenarios and implications for ecosystem function. Polar Res. 34,
762 24252. doi:10.3402/polar.v34.24252

763 Fisher, N.S., Burns, K.A., Cherry, R.D., Heyraud, M., 1983. Accumulation and cellular
764 distribution of ^{241}Am, ^{210}Po and ^{210}Pb in two marine algae. Mar. Ecol. Prog. Ser.
765 11, 233–237.

766 Fleer, A.P., Bacon, M.P., 1984. Determination of ^{210}Pb and ^{210}Po in seawater and
767 marine particulate matter. Nucl. Instruments Methods Phys. Res. 223, 243–249.
768 doi:10.1016/0167-5087(84)90655-0

769 Flynn, W.W., 1968. The determination of low levels of polonium-210 in environmental
770 materials. Anal. Chim. Acta 43, 221–227.

771 Forest, A., Sampei, M., Hattori, H., Makabe, R., Sasaki, H., Fukuchi, M., Wassmann,
772 P., Fortier, L., 2007. Particulate organic carbon fluxes on the slope of the
773 Mackenzie Shelf (Beaufort Sea): Physical and biological forcing of shelf-basin
774 exchanges. J. Mar. Syst. 68, 39–54. doi:10.1016/j.jmarsys.2006.10.008

775 Friedrich, J., 2011. Polonium-210 and Lead-210 activities measured on 17 water bottle
776 profiles and 50 surface water samples during POLARSTERN cruise ARK-XXII/2.
777 Alfred Wegener Institute, Helmholtz Cent. Polar Mar. Res. Bremerhaven.
778 doi:10.1594/PANGAEA.763937

779 Friedrich, J., Rutgers van der Loeff, M.M., 2002. A two-tracer (^{210}Po–^{234}Th) approach
780 to distinguish organic carbon and biogenic silica export flux in the Antarctic
781 Circumpolar Current. Deep Sea Res. Part I Oceanogr. Res. Pap. 49, 101–120.
782 doi:10.1016/S0967-0637(01)00045-0

783 Frigstad, H., Andersen, T., Bellerby, R.G.J., Silyakova, A., Hessen, D.O., 2014.
784 Variation in the seston C:N ratio of the Arctic Ocean and pan-Arctic shelves. J.
785 Mar. Syst. 129, 214–223. doi:10.1016/j.jmarsys.2013.06.004

786 Haas, C., Pfaffling, A., Hendricks, S., Rabenstein, L., Etienne, J.-L., Rigor, I., 2008.
787 Reduced ice thickness in Arctic Transpolar Drift favors rapid ice retreat. Geophys.
788 Res. Lett. 35, L17501. doi:10.1029/2008GL034457

789 Haine, T.W.N., Curry, B., Gerdes, R., Hansen, E., Karcher, M., Lee, C., Rudels, B.,
790 Spreen, G., de Steur, L., Stewart, K.D., Woodgate, R., 2015. Arctic freshwater
791 export: Status, mechanisms, and prospects. Glob. Planet. Change 125, 13–35.
792 doi:10.1016/j.gloplacha.2014.11.013

793 Honjo, S., Krishfield, R.A., Eglinton, T.I., Manganini, S.J., Kemp, J.N., Doherty, K.,
794 Hwang, J., McKee, T.K., Takizawa, T., 2010. Biological pump processes in the
795 cryopelagic and hemipelagic Arctic Ocean: Canada Basin and Chukchi Rise. Prog.
796 Oceanogr. 85, 137–170. doi:10.1016/j.pocean.2010.02.009

797 Hu, W., Chen, M., Yang, W., Zhang, R., Qiu, Y., Zheng, M., 2014. Low ^{210}Pb in the
798 upper thermocline in the Canadian Basin: scavenge process over the Chukchi Sea.
799 Acta Oceanol. Sin. 33, 28–39. doi:10.1007/s13131-014-0486-6

800 Huh, C.-A., Pisias, N.G., Kelley, J.M., Maiti, T.C., Grantz, A., 1997. Natural
801 radionuclides and plutonium in sediments from the western Arctic Ocean:
802 sedimentation rates and pathways of radionuclides. Deep Sea Res. Part II Top.
803 Stud. Oceanogr. 44, 1725–1743. doi:10.1016/S0967-0645(97)00040-4

804 Kawaguchi, Y., Hutchings, J.K., Kikuchi, T., Morison, J.H., Krishfield, R.A., 2012.
805 Anomalous sea-ice reduction in the Eurasian Basin of the Arctic Ocean during
806 summer 2010. Polar Sci. 6, 39–53. doi:10.1016/j.polar.2011.11.003

807 Kim, G., Church, T.M., 2001. Seasonal biogeochemical fluxes of ^{234}Th and ^{210}Po in the
808 Upper Sargasso Sea: Influence from atmospheric iron deposition. Global
809 Biogeochem. Cycles 15, 651–661. doi:10.1029/2000GB001313

810 Klunder, M.B., Bauch, D., Laan, P., de Baar, H.J.W., van Heuven, S., Ober, S., 2012.
811 Dissolved iron in the Arctic shelf seas and surface waters of the central Arctic
812 Ocean: Impact of Arctic river water and ice-melt. J. Geophys. Res. Ocean. 117,
813 C01027. doi:10.1029/2011JC007133

814 Korhonen, M., Rudels, B., Marnela, M., Wisotzki, A., Zhao, J., 2013. Time and space
815 variability of freshwater content, heat content and seasonal ice melt in the Arctic
816 Ocean from 1991 to 2011. Ocean Sci. 9, 1015–1055. doi:10.5194/os-9-1015-2013

817 Kramer, M., Kiko, R., 2011. Brackish meltponds on Arctic sea ice—a new habitat for
818 marine metazoans. Polar Biol. 34, 603–608. doi:10.1007/s00300-010-0911-z

819 Kwok, R., Cunningham, G.F., Wensnahan, M., Rigor, I., Zwally, H.J., Yi, D., 2009.
820 Thinning and volume loss of the Arctic Ocean sea ice cover: 2003–2008. J.
821 Geophys. Res. 114, C07005. doi:10.1029/2009JC005312

822 Laan, P., Ober, S., Boom, L., Bakker, K., 2008. Hydrochemistry measured on water
823 bottle samples during POLARSTERN cruise ARK-XXII/2 (SPACE). R.
824 Netherlands Inst. Sea Res. Texel. doi:10.1594/PANGAEA.708642

825 Lalande, C., Bélanger, S., Fortier, L., 2009a. Impact of a decreasing sea ice cover on the

826 vertical export of particulate organic carbon in the northern Laptev Sea, Siberian
827 Arctic Ocean. Geophys. Res. Lett. 36, L21604. doi:10.1029/2009GL040570

828 Lalande, C., Forest, A., Barber, D.G., Gratton, Y., Fortier, L., 2009b. Variability in the
829 annual cycle of vertical particulate organic carbon export on Arctic shelves:
830 Contrasting the Laptev Sea, Northern Baffin Bay and the Beaufort Sea. Cont. Shelf
831 Res. 29, 2157–2165. doi:10.1016/j.csr.2009.08.009

832 Lalande, C., Moran, S.B., Wassmann, P., Grebmeier, J.M., Cooper, L.W., 2008. ^{234}Th-
833 derived particulate organic carbon fluxes in the northern Barents Sea with
834 comparison to drifting sediment trap fluxes. J. Mar. Syst. 73, 103–113.
835 doi:10.1016/j.jmarsys.2007.09.004

836 Lam, P.J., Marchal, O., 2015. Insights into Particle Cycling from Thorium and Particle
837 Data. Ann. Rev. Mar. Sci. 7, 159–184. doi:10.1146/annurev-marine-010814-
838 015623

839 Laxon, S.W., Giles, K.A., Ridout, A.L., Wingham, D.J., Willatt, R., Cullen, R., Kwok,
840 R., Schweiger, A., Zhang, J., Haas, C., Hendricks, S., Krishfield, R., Kurtz, N.,
841 Farrell, S., Davidson, M., 2013. CryoSat-2 estimates of Arctic sea ice thickness
842 and volume. Geophys. Res. Lett. 40, 732–737. doi:10.1002/grl.50193

843 Le Fouest, V., Babin, M., Tremblay, J.-É., 2013. The fate of riverine nutrients on Arctic
844 shelves. Biogeosciences 10, 3661– 3677. doi:10.5194/bg-10-3661-2013

845 Lepore, K., Moran, S.B., Smith, J.N., 2009. ^{210}Pb as a tracer of shelf–basin transport
846 and sediment focusing in the Chukchi Sea. Deep Sea Res. Part II Top. Stud.
847 Oceanogr. 56, 1305–1315. doi:10.1016/j.dsr2.2008.10.021

848 Ma, Q., Chen, M., Qiu, Y., Li, Y., 2005. Regional estimates of POC export flux derived
849 from thorium-234 in the western Arctic Ocean. Acta Oceanol. Sin. 24, 97–108.

850 Masqué, P., Cochran, J.K., Hirschberg, D.J., Dethleff, D., Hebbeln, D., Winkler, A.,
851 Pfirman, S., 2007. Radionuclides in Arctic sea ice: Tracers of sources, fates and ice
852 transit time scales. Deep Sea Res. Part I Oceanogr. Res. Pap. 54, 1289–1310.
853 doi:10.1016/j.dsr.2007.04.016

854 Masqué, P., Sanchez-Cabeza, J.A., Bruach, J.M., Palacios, E., Canals, M., 2002.
855 Balance and residence times of ^{210}Pb and ^{210}Po in surface waters of the
856 northwestern Mediterranean Sea. Cont. Shelf Res. 22, 2127–2146.
857 doi:10.1016/S0278-4343(02)00074-2

858 Middag, R., de Baar, H.J.W., Laan, P., Bakker, K., 2009. Dissolved aluminium and the
859 silicon cycle in the Arctic Ocean. Mar. Chem. 115, 176–195.
860 doi:10.1016/j.marchem.2009.08.002

861 Moore, R.M., Smith, J.N., 1986. Disequilibria between ^{226}Ra, ^{210}Pb and ^{210}Po in the
862 Arctic Ocean and the implications for chemical modification of the Pacific water
863 inflow. Earth Planet. Sci. Lett. 77, 285–292. doi:10.1016/0012-821X(86)90140-8

864 Nozaki, Y., Dobashi, F., Kato, Y., Yamamoto, Y., 1998. Distribution of Ra isotopes and
865 the ^{210}Pb and ^{210}Po balance in surface seawaters of the mid Northern Hemisphere.

866 Deep Sea Res. Part I Oceanogr. Res. Pap. 45, 1263–1284. doi:10.1016/S0967-
867 0637(98)00016-8

868 Nozaki, Y., Ikuta, N., Yashima, M., 1990. Unusually large ^{210}Po deficiencies relative to
869 ^{210}Pb in the Kuroshio Current of the East China and Philippine seas. J. Geophys.
870 Res. 95, 5321. doi:10.1029/JC095iC04p05321

871 Nozaki, Y., Thomson, J., Turekian, K.K., 1976. The distribution of ^{210}Pb and ^{210}Po in
872 the surface waters of the Pacific Ocean. Earth Planet. Sci. Lett. 32, 304–312.
873 doi:10.1016/0012-821X(76)90070-4

874 Nozaki, Y., Turekian, K.K., Von Damm, K., 1980. ^{210}Pb in GEOSECS water profiles
875 from the North Pacific. Earth Planet. Sci. Lett. 49, 393–400. doi:10.1016/0012-
876 821X(80)90081-3

877 Nozaki, Y., Zhang, J., Takeda, A., 1997. ^{210}Pb and ^{210}Po in the equatorial Pacific and
878 the Bering Sea: the effects of biological productivity and boundary scavenging.
879 Deep Sea Res. Part II Top. Stud. Oceanogr. 44, 2203–2220. doi:10.1016/S0967-
880 0645(97)00024-6

881 O'Brien, M.C., Melling, H., Pedersen, T.F., Macdonald, R.W., 2013. The role of eddies
882 on particle flux in the Canada Basin of the Arctic Ocean. Deep Sea Res. Part I
883 Oceanogr. Res. Pap. 71, 1–20. doi:10.1016/j.dsr.2012.10.004

884 Parkinson, C.L., Comiso, J.C., 2013. On the 2012 record low Arctic sea ice cover:
885 Combined impact of preconditioning and an August storm. Geophys. Res. Lett. 40,
886 1356–1361. doi:10.1002/grl.50349

887 Quigley, M.S., Santschi, P.H., Hung, C.-C., Guo, L., Honeyman, B.D., 2002.
888 Importance of acid polysaccharides for ^{234}Th complexation to marine organic
889 matter. Limnol. Oceanogr. 47, 367–377. doi:10.4319/lo.2002.47.2.0367

890 Rabe, B., Karcher, M., Kauker, F., Schauer, U., Toole, J.M., Krishfield, R.A., Pisarev,
891 S., Kikuchi, T., Su, J., 2014. Arctic Ocean basin liquid freshwater storage trend
892 1992-2012. Geophys. Res. Lett. 41, 961–968. doi:10.1002/2013GL058121

893 Rabe, B., Karcher, M., Schauer, U., Toole, J.M., Krishfield, R.A., Pisarev, S., Kauker,
894 F., Gerdes, R., Kikuchi, T., 2011. An assessment of Arctic Ocean freshwater
895 content changes from the 1990s to the 2006–2008 period. Deep Sea Res. Part I
896 Oceanogr. Res. Pap. 58, 173–185. doi:10.1016/j.dsr.2010.12.002

897 Rachold, V., Alabyan, A., Hubberten, H.-W., Korotaev, V.N., Zaitsev, A.A., 1996.
898 Sediment transport to the Laptev Sea-hydrology and geochemistry of the Lena
899 River. Polar Res. 15, 183–196. doi:10.1111/j.1751-8369.1996.tb00468.x

900 Randelhoff, A., Guthrie, J.D., 2016. Regional patterns in current and future export
901 production in the central Arctic Ocean quantified from nitrate fluxes. Geophys.
902 Res. Lett. 43, 8600–8608. doi:10.1002/2016GL070252

903 Redfield, A.C., Ketchum, B.H., Richards, F.A., 1963. The influence of organisms on
904 the composition of sea-water, in: Hill, M.N. (Ed.), The Sea: Ideas and
905 Observations on Progress in the Study of the Seas. Wiley Interscience, New York,

pp. 26–77.

Reiniger, R.F., Ross, C.K., 1968. A method of interpolation with application to oceanographic data. Deep Sea Res. Oceanogr. Abstr. 15, 185–193. doi:10.1016/0011-7471(68)90040-5

Renner, A.H.H., Gerland, S., Haas, C., Spreen, G., Beckers, J.F., Hansen, E., Nicolaus, M., Goodwin, H., 2014. Evidence of Arctic sea ice thinning from direct observations. Geophys. Res. Lett. 41, 5029–5036. doi:10.1002/2014GL060369

Roberts, K.A., Cochran, J.K., Barnes, C., 1997. ^{210}Pb and ^{239,240}Pu in the Northeast Water Polynya, Greenland: particle dynamics and sediment mixing rates. J. Mar. Syst. 10, 401–413. doi:10.1016/S0924-7963(96)00061-9

Roca-Martí, M., Puigcorbé, V., Rutgers van der Loeff, M.M., Katlein, C., Fernández-Méndez, M., Peeken, I., Masqué, P., 2016. Carbon export fluxes and export efficiency in the central Arctic during the record sea-ice minimum in 2012: a joint ^{234}Th/^{238}U and ^{210}Po/^{210}Pb study. J. Geophys. Res. Ocean. 121, 5030–5049. doi:10.1002/2016JC011816

Rodriguez y Baena, A.M., Fowler, S.W., Miquel, J.C., 2007. Particulate organic carbon: natural radionuclide ratios in zooplankton and their freshly produced fecal pellets from the NW Mediterranean (MedFlux 2005). Limnol. Oceanogr. 52, 966–974. doi:10.4319/lo.2007.52.3.0966

Roeske, T., Bauch, D., Rutgers van der Loeff, M., Rabe, B., 2012. Utility of dissolved barium in distinguishing North American from Eurasian runoff in the Arctic Ocean. Mar. Chem. 132–133, 1–14. doi:10.1016/j.marchem.2012.01.007

Rudels, B., 2009. Arctic Ocean Circulation, in: Steele, J.H., Thorpe, S.A., Turekian, K.K. (Eds.), Ocean Currents: A Derivative of the Encyclopedia of Ocean Sciences. Academic Press, London, pp. 211–225.

Rudels, B., Anderson, L.G., Jones, E.P., 1996. Formation and evolution of the surface mixed layer and halocline of the Arctic Ocean. J. Geophys. Res. Ocean. 101, 8807–8821. doi:10.1029/96JC00143

Rudels, B., Jones, E.P., Schauer, U., Eriksson, P., 2004. Atlantic sources of the Arctic Ocean surface and halocline waters. Polar Res. 23, 181–208. doi:10.1111/j.1751-8369.2004.tb00007.x

Rutgers van der Loeff, M., Cai, P., Stimac, I., Bauch, D., Hanfland, C., Roeske, T., Moran, S.B., 2012. Shelf-basin exchange times of Arctic surface waters estimated from ^{228}Th/^{228}Ra disequilibrium. J. Geophys. Res. Ocean. 117, C03024. doi:10.1029/2011JC007478

Rutgers van der Loeff, M., Kipp, L., Charette, M.A., Moore, W.S., Black, E., Stimac, I., Charkin, A., Bauch, D., Valk, O., Karcher, M., Krumpen, T., Casacuberta, N., Smethie, W., Rember, R., 2018. Radium Isotopes across the Arctic Ocean show Time Scales of Water Mass Ventilation and Increasing Shelf Inputs. J. Geophys. Res. Ocean. doi:10.1029/2018JC013888

946 Sarin, M.M., Krishnaswami, S., Ramesh, R., Somayajulu, B.L.K., 1994. ^{238}U decay
947 series nuclides in the northeastern Arabian Sea: Scavenging rates and cycling
948 processes. Cont. Shelf Res. 14, 251–265. doi:10.1016/0278-4343(94)90015-9

949 Schauer, U., 2008. The expedition ARKTIS-XXII/2 of the research vessel "Polarstern"
950 in 2007. Reports on polar and marine research 579. Bremerhaven.

951 Schauer, U., Wisotzki, A., 2010. Physical oceanography during POLARSTERN cruise
952 ARK-XXII/2 (SPACE). Alfred Wegener Institute, Helmholtz Cent. Polar Mar.
953 Res. Bremerhaven. doi:10.1594/PANGAEA.733418

954 Shannon, L.V., Cherry, R.D., Orren, M.J., 1970. Polonium-210 and lead-210 in the
955 marine environment. Geochim. Cosmochim. Acta 34, 701–711. doi:10.1016/0016-
956 7037(70)90072-4

957 Shaw, W.J., Stanton, T.P., McPhee, M.G., Morison, J.H., Martinson, D.G., 2009. Role
958 of the upper ocean in the energy budget of Arctic sea ice during SHEBA. J.
959 Geophys. Res. 114, C06012. doi:10.1029/2008JC004991

960 Smith, J.N., Ellis, K.M., 1995. Radionuclide tracer profiles at the CESAR Ice Station
961 and Canadian Ice Island in the western Arctic Ocean. Deep Sea Res. Part II Top.
962 Stud. Oceanogr. 42, 1449–1470. doi:10.1016/0967-0645(95)00049-6

963 Smith, J.N., Moran, S.B., Macdonald, R.W., 2003. Shelf–basin interactions in the Arctic
964 Ocean based on ^{210}Pb and Ra isotope tracer distributions. Deep Sea Res. Part I
965 Oceanogr. Res. Pap. 50, 397–416. doi:10.1016/S0967-0637(02)00166-8

966 Stewart, G., Cochran, J.K., Miquel, J.C., Masqué, P., Szlosek, J., Rodriguez y Baena,
967 A.M., Fowler, S.W., Gasser, B., Hirschberg, D.J., 2007a. Comparing POC export
968 from ^{234}Th/^{238}U and ^{210}Po/^{210}Pb disequilibria with estimates from sediment traps in
969 the northwest Mediterranean. Deep Sea Res. Part I Oceanogr. Res. Pap. 54, 1549–
970 1570. doi:10.1016/j.dsr.2007.06.005

971 Stewart, G., Cochran, J.K., Xue, J., Lee, C., Wakeham, S.G., Armstrong, R.A., Masqué,
972 P., Carlos Miquel, J., 2007b. Exploring the connection between ^{210}Po and organic
973 matter in the northwestern Mediterranean. Deep Sea Res. Part I Oceanogr. Res.
974 Pap. 54, 415–427. doi:10.1016/j.dsr.2006.12.006

975 Stewart, G., Fisher, N.S., 2003. Bioaccumulation of polonium-210 in marine copepods.
976 Limnol. Oceanogr. 48, 2011–2019. doi:10.4319/lo.2003.48.5.2011

977 Stewart, G., Fowler, S., Teyssié, J.L., Cotret, O., Cochran, J.K., Fisher, N.S., 2005.
978 Contrasting transfer of polonium-210 and lead-210 across three trophic levels in
979 marine plankton. Mar. Ecol. Prog. Ser. 290, 27–33. doi:10.3354/meps290027

980 Stewart, G., Moran, S.B., Lomas, M.W., 2010. Seasonal POC fluxes at BATS estimated
981 from ^{210}Po deficits. Deep Sea Res. Part I Oceanogr. Res. Pap. 57, 113–124.
982 doi:10.1016/j.dsr.2009.09.007

983 Stroeve, J.C., Serreze, M.C., Holland, M.M., Kay, J.E., Malanik, J., Barrett, A.P., 2012.
984 The Arctic's rapidly shrinking sea ice cover: a research synthesis. Clim. Change
985 110, 1005–1027. doi:10.1007/s10584-011-0101-1

Tateda, Y., Carvalho, F.P., Fowler, S.W., Miquel, J.-C., 2003. Fractionation of ^{210}Po and ^{210}Pb in coastal waters of the NW Mediterranean continental margin. Cont. Shelf Res. 23, 295–316. doi:10.1016/S0278-4343(02)00167-X

Thomson, J., Turekian, K.K., 1976. ^{210}Po and ^{210}Pb distributions in ocean water profiles from the Eastern South Pacific. Earth Planet. Sci. Lett. 32, 297–303. doi:10.1016/0012-821X(76)90069-8

Tremblay, J.-É., Anderson, L.G., Matrai, P., Coupel, P., Bélanger, S., Michel, C., Reigstad, M., 2015. Global and regional drivers of nutrient supply, primary production and CO_2 drawdown in the changing Arctic Ocean. Prog. Oceanogr. 139, 171–196. doi:10.1016/j.pocean.2015.08.009

Ulfsbo, A., Cassar, N., Korhonen, M., van Heuven, S., Hoppema, M., Kattner, G., Anderson, L.G., 2014. Late summer net community production in the central Arctic Ocean using multiple approaches. Global Biogeochem. Cycles 28, 1129–1148. doi:10.1002/2014GB004833

Verdeny, E., Masqué, P., Garcia-Orellana, J., Hanfland, C., Cochran, J.K., Stewart, G., 2009. POC export from ocean surface waters by means of ^{234}Th/^{238}U and ^{210}Po/^{210}Pb disequilibria: A review of the use of two radiotracer pairs. Deep Sea Res. Part II Top. Stud. Oceanogr. 56, 1502–1518. doi:10.1016/j.dsr2.2008.12.018

Wassmann, P., 2011. Arctic marine ecosystems in an era of rapid climate change. Prog. Oceanogr. 90, 1–17. doi:10.1016/j.pocean.2011.02.002

Wassmann, P., Bauerfeind, E., Fortier, M., Fukuchi, M., Hargrave, B., Moran, B., Noji, T., Nöthig, E.-M., Olli, K., Peinert, R., Sasaki, H., Shevchenko, V., 2004. Particulate organic carbon flux to the Arctic ocean sea floor, in: Stein, R., Macdonald, R.W. (Eds.), The Organic Carbon Cycle in the Arctic Ocean. Springer Berlin Heidelberg, Berlin, pp. 101–138. doi:10.1007/978-3-642-18912-8_5

Wassmann, P., Duarte, C.M., Agustí, S., Sejr, M.K., 2011. Footprints of climate change in the Arctic marine ecosystem. Glob. Chang. Biol. 17, 1235–1249. doi:10.1111/j.1365-2486.2010.02311.x

Wassmann, P., Reigstad, M., 2011. Future Arctic Ocean Seasonal Ice Zones and Implications for Pelagic-Benthic Coupling. Oceanography 24, 220–231. doi:10.5670/oceanog.2011.74

Wiedmann, I., Reigstad, M., Sundfjord, A., Basedow, S., 2014. Potential drivers of sinking particle's size spectra and vertical flux of particulate organic carbon (POC): Turbulence, phytoplankton, and zooplankton. J. Geophys. Res. Ocean. 119, 6900–6917. doi:10.1002/2013JC009754

Wisotzki, A., Bakker, K., 2008. Hydrochemistry measured on water bottle samples during POLARSTERN cruise ARK-XXII/2. Alfred Wegener Institute, Helmholtz Cent. Polar Mar. Res. Bremerhaven. doi:10.1594/PANGAEA.759286